Chronopharmacological Study of Interferon-β in Mice : Relationship Between Diurnal Rhythm of Pharmacological Effect Induced by Receptor-Mediated Drugs and Their Receptor Expression on Target Tissue

髙根, 浩
九州大学薬学研究科医療薬学専攻

https://doi.org/10.11501/3180246

出版情報：九州大学, 2000, 博士（薬学）, 課程博士
バージョン：
権利関係：

Doctoral Dissertation

Chronopharmacological Study of Interferon-β in Mice

Relationship Between Diurnal Rhythm of Pharmacological Effect Induced by Receptor-Mediated Drugs and Their Receptor Expression on Target Tissue

Department of Clinical Pharmacokinetics, Division of Pharmaceutical Sciences,

Graduate School, Kyushu University

Hiroshi Takane

2001

Doctoral Dissertation

Chronopharmacological Study of Interferon-β in Mice

Relationship Between Diurnal Rhythm of Pharmacological Effect Induced by Receptor-Mediated Drugs and Their Receptor Expression on Target Tissue

Department of Clinical Pharmacokinetics, Division of Pharmaceutical Sciences,

Graduate School, Kyushu University

Hiroshi Takane

2001

Contents

Contents i
Introduction ii
Abbreviations vii
Released articles viii

Chapter 1 Influence of IFN-β Dosing Time on Its Pharmacological Effects in Mice

1-1 Influence of IFN-β Dosing Time on Antitumor Effect in Tumor-Bearing Mice

Abstract 1
Materials and Methods 2
Results 6
Discussion 9
Tables & Figures 12

1-2 Influence of IFN-β Dosing Time on Antiviral Effect in Mice

Abstract 19
Materials and Methods 20
Results 24
Discussion 26
Tables & Figures 29

Chapter 2 Influence of EPO Dosing Time on Erythropoietic Effect in Mice

Abstract 34
Materials and Methods 35
Results 39
Discussion 42
Tables & Figures 45

Summary 50

References 53

Introduction

1. Chronopharmacology and Chronopharmacotherapy

A diurnal rhythm has been demonstrated for a large number of physiological functions (Lévi et al., 1991; Refinetti and Menaker, 1992; Burgess et al., 1997). Circadian oscillator in mammal is located in the suprachiasmatic nuclei (SCN) of hypothalamus and plays a critical role in adapting endogenous physiological functions to cyclic environmental factors such as light, temperature and social communication. Moreover, the risk and/or intensity of the symptoms of disease vary predictably with twenty four hour cycle. For example, the frequency of asthmatic episodes increase from evening to early morning, because of diurnal rhythms in airway potency, bronchial responsiveness and release of inflammatory (Goldenheim and Schein, 1992). Therefore, evening dosing with theophylline produces a significant improvement in nocturnal asthmatic symptoms (Rivington et al., 1985; Goldenheim and Schein, 1992). The evening dosing with H_2 receptor antagonist is more benefit regimen in peptic ulcer therapy, because there is a significant diurnal rhythm with high acid production in the evening and low in the morning (Warner and McIsaac, 1992). On the other hand, responses to a variety of drugs show diurnal rhythmicity (Ohdo et al., 1988, 1991, 1996, 1998; Watanabe et al., 1992). Use of a chronopharmacological strategy can improve tumor response to treatment, and overall survival rates and reduce drug toxicities in humans (Hrushesky, 1985; Lévi et al., 1997). The leukocyte-increasing effect of granulocyte colony-stimulating factor, which one of hematopoietic factors, varies depending on dosing time (Ohdo et al., 1998). The mechanisms involved in the diurnal rhythm of drug susceptibility have been examined from the viewpoints of the sensitivity of living organisms to drugs and/or the pharmacokinetics of drugs.

2. Diurnal Rhythm of Receptor Expression and Pharmacological Effect Induced by Receptor-Mediated Drug

Previous studies have demonstrated that the number in receptor of neurotransmitters such as adrenaline (Kafka et al., 1981), dopamine (Naber et al., 1980) benzodiazepine (Kafka et al., 1986) and acetylcholine (Kafka et al., 1986) shows a significant diurnal rhythm. Rhythms in brain neurotransmitter receptor may contribute to the behavioral rhythm of active and rest period. SCN lesion disappears a diurnal rhythm in number of brain receptors (Kafka et al.,

1985). Thus, SCN may play in the central pacemaking function of a diurnal rhythm in receptor expression on brain. Also, chronic administration of clorgyline (Wirz-Justice et al., 1982), lithium (Kafka et al., 1982) or imipramine (Wirz-Justice et al., 1980) can delay the phase-position or abolish the diurnal rhythm of brain receptors. On the other hand, the higher analgesic effectiveness of morphine is observed after drug injection during the dark phase in mice (Kavaliers and Hirst, 1983). The opiate receptor binding is significant diurnal rhythm with a higher level during the dark phase (Naber et al., 1981). However, little is known about the relationship between the diurnal rhythm of pharmacological effect induced by receptor-mediated drugs and their receptor expression on target tissues. Also, previous study has shown that the interindividual variability in response of β-adrenoreceptor agonist or antagonist can be explained by that in β-adrenoreceptor density on lymphocytes (Fraser et al., 1981, Zhou et al., 1989). Therefore, the rhythmic change of receptor expression may mainly contribute to that of effect induced by receptor-mediated drug.

In this study, I investigated the influence of dosing time on pharmacological effects of receptor-mediated drugs such as interferon-β (IFN-β) and erythropoietin (EPO) in mice, and the relationship between the diurnal rhythm of pharmacological effect induced by receptor-mediated drugs and their receptor expression on target tissue. Additionally, I discussed about the usefulness of clinical chronotherapy with receptor-mediated drugs.

3.1. Influence of IFN-β Dosing Time on Antitumor Effect in Tumor-Bearing Mice

IFNs are multifunctional cytokines that have not only antiproliferative and immunological effects but also potent antiviral effects (Baron et al., 1991). IFNs have been widely used to treat patients with various cancer and hepatitis. However, adverse effects such as fever, headache, leukopenia and thrombocytopenia are frequently observed in patients treated with IFNs (Baron et al., 1991). One approach to increasing the efficiency of IFNs treatment is to administer the drugs at a time when they are most effective and/or tolerated. Certainly, the fever (Koyanagi et al., 1997; Ohdo et al., 1997a) or leukopenia (Koren and Fleischmann, 1993) induced by IFN-α is significantly affected by dosing time. Also, the antitumor activity of IFN-α and -γ varies depending on dosing time in a mouse model (Koren et al., 1993). Such

dosing time-dependent differences could occur at many levels, including dosing time-dependent variation in pharmacokinetics, tumor responsiveness and host immune responsiveness. However, the exact mechanisms have not been clarified yet.

IFNs inhibit cell growth through the upregulation of p21 wild-type p53-activated fragment 1 (p21WAF1) which is cyclin-dependent kinase (cdk) inhibitor (Sangfelt et al, 1997; Mandal et al, 1998). IFNs elicit the transcription of various genes through activation of signal transducers and activators of transcription 1 (STAT1) protein, via binding to specific receptors (Darnell et al., 1994). Although a significant dosing time-dependent pharmacokinetics has been demonstrated for IFNs concentration in plasma, it has not been systematically investigated in tissue. This is because it is often difficult to obtain the time course of drug concentrations in tissue from individual subjects. NONMEM (non-linear mixed effect model) is a computer program designed to analyze pharmacokinetics in study populations by pooling data. In this study, NONMEM was applied to the pharmacokinetic analysis of IFN-β concentrations in tumor mass.

The purpose of this section was to investigate the influence of dosing time on tumor growth following the intratumoral administration of IFN-β in tumor-bearing mice. The mechanism underlying the dosing time-dependent difference was elucidated based on IFN-β pharmacodynamics or pharmacokinetics.

3.2. Influence of IFN-β Dosing Time on Antiviral Effect in Mice

IFN elicits biological activity through binding to specific receptors (Darnell et al., 1994). IFN-α and -β bind equally to IFN-α/β receptor (IFNAR) (Novick et al, 1994). IFN-α and -β are the only effective antiviral agent that eliminates hepatitis virus from hepatocytes. However, only about half of patients with hepatitis C virus (HCV) infection receiving IFN-α therapy are able to eliminate virus or normalize serum aminotransferase (Davis et al., 1989; Lin et al., 1995). The response to IFN-α therapy is associated with a amount of serum HCV-RNA (Toyoda et al., 1997) and HCV genotype (Kanai et al., 1992). Furthermore, the expression of IFNAR in liver is significantly related to the response to IFN therapy (Mizukoshi et al., 1998; Yatsuhashi et al., 1999). Therefore, the inter or intraindividual variability of IFNAR level may be important host factor influencing the response to IFN-α and -β. On the other hand,

adverse effects such as fever and headache, leukopenia and thrombocytopenia are frequently observed in patients treated with IFNs (Baron et al., 1991). In particular, fever is a frequent side effect in patients with IFN therapy.

In general, the rhythmic change of drug response is caused by that of pharmacokinetic factors such as drug concentration at the site of action and/or pharmacodynamic factors such as receptor sensitivity to drug. The diurnal rhythm in myelosuppressive toxicity of anticancer drugs is closely related to that in cell cycle distribution of bone marrow cells (Ohdo et al., 1997b, Tampellini et al., 1998). One approach to increase the efficiency of IFNs treatment is the administration of the drugs at the time that they are best effective and/or tolerated. Certainly, the fever (Koyanagi et al., 1997; Ohdo et al., 1997a) or antiviral activity (Koyanagi et al., 1997) induced by IFN-α is significantly affected by dosing time. However, the exact mechanisms have not been clarified yet.

In this section, I examined the influence of IFN-β dosing time on antiviral activity and fever in mice and the relationship between the diurnal rhythm of pharmacological effect induced by IFN-β and IFNAR expression.

3.3. Influence of EPO Dosing Time on Erythropoietic Effect in Mice

EPO is the glycoprotein cytokine responsible for the primary regulation of erythroid cell maturation, and elicits the survival and proliferation of erythroid progenitor in bone marrow through the induction of antiapotosis-regulatory gene, via binding to erythropoietin receptor (EPOR). EPO is synthesized by cells adjacent to the proximal renal tubules in response to signal from a renal oxygen-sensing device (Goldberg et al., 1988). Since EPO gene was cloned, its recombinant product have been used to treat patients with hematological disease such as anemia by chronic renal failure.

Previous clinical study has shown a strategy for success of EPO-replacement treatment in patients with chronic renal disease. The subcutaneous administration of EPO is more convenient for patients than the intravenous administration (Eschbach et al., 1989). Subcutaneous injections is more sustained plasma level, resulting in slow release from subcutaneous depots (McMahon et al., 1990). Also, EPO given within an interval of 72 hr was more effective in stimulating erythropoiesis than administration within 24 hr interval for the

same total dose (Breymann et al., 1996). On the other hand, hypertension are frequently observed in patients treated with EPO. The hypertension is due to a rapid increase of hematocrit. EPO treatment for patient undergoing renal dialysis is expensive on the order of $10,000 per year (Doolittle, 1991). By considering those findings, the use of lower dosage and slower but possible safer increase of hematocrit are recommended in the EPO-replacement strategy.

In general, the rhythmic change of drug response is caused by that of pharmacokinetic factors such as drug concentration at the site of action and/or pharmacodynamic factors such as receptor sensitivity to drug. The leukocyte-increasing effect of granulocyte colony-stimulating factor (G-CSF), which one of hematopoietic factors, varies depending on dosing time (Ohdo et al., 1998). The rhythmicity of G-CSF effect is due to that in sensitivity of bone marrow cells to G-CSF. However, the chronopharmacological study of EPO has not been performed yet in detail. The clinical chronotherapy with EPO may be useful for patients receiving EPO therapy.

This section was designed to examine the existence of dosing time-dependence on the erythropoietic effect of EPO in mice. The mechanism underlying the dosing time-dependent difference was investigated from viewpoints of EPO pharmacodynamics and/or pharmacokinetics.

Abbreviations

SCN; suprachiasmatic nuclei
IFN-β; interferon-β;
IFNAR; interferon-α/β receptor
p21WAF1; p21 wild-type p53-activated fragment 1
cdk; cyclin-dependent kinase
STAT1; signal transducers and activators of transcription 1
ISGF-3; interferon-stimulated gene factor-3
ISRE; interferon-stimulated response element
NONMEM; non-linear mixed effect model
CL; clearance
Vc; central volume of distribution
k12; distribution rate constant from central to peripheral compartment
k21; distribution rate constant from peripheral to central compartment
AUC; area under the curve
MRT; mean residence time
ANOVA; analysis of variance
2', 5'-OAS; 2', 5'-oligoadenylate synthetase
Kd; dissociation constant
HCV; hepatitis C virus
PGE_2; prostagrandin E_2
COX-2; cyclooxygenase-2
interleukin; IL
EPO; erythropoietin
EPOR; erythropoietin receptor
CFU-E; colony-forming units-erythroid
ka; absorption rate constant
ke; elimination rate constant
F; bioavailability
Cmax; peak plasma concentration

Released Articles

1) Takane H, Ohdo S, Yamada T, Yukawa E and Higuchi S (2000) Chronopharmacology of antitumor effect induced by interferon-β in tumor-bearing mice. J Pharmacol Exp Ther 294: 746-752.

2) Takane H, Ohdo S, Yamada T, Koyanagi S, Yukawa E and Higuchi S (2001) Relationship between diurnal rhythm of cell cycle and interferon receptor expression in implanted-tumor cells. Life Sci 68: 1449-1455.

3) Ohdo S, Wang D-S, Koyanagi S, Takane H, Inoue K, Aramaki H, Yukawa E and Higuchi S (2000) Basis for dosing time-dependent changes in the antiviral activity of interferon-α in mice. J Pharmacol Exp Ther 294: 488-493.

4) Wang D-S, Ohdo S, Koyanagi S, Takane H, Aramaki H, Yukawa E and Higuchi S (2001) Effect of dosing schedule on pharmacokinetics of alpha interferon and anti-alpha interferon neutralizing antibody in mice. Antimicrob Agents Chemother 45: 176-180.

Chapter 1

Influence of IFN-β Dosing Time on Its Pharmacological Effects in Mice

1-1 Influence of IFN-β Dosing Time on Antitumor Effect in Tumor-Bearing Mice

Abstract

The mechanisms underlying the dosing time-dependent change in the antitumor effect of IFN-β were investigated based on the sensitivity of tumor cells and the pharmacokinetics of the drug. Tumor-bearing mice were housed under standardized light-dark cycle conditions (lights on at 07:00, off at 19:00) with food and water available *ad libitum*. The antitumor effect of IFN-β (0.5 MIU/kg, intratumoral (i.t.)) was more efficient in early light phase than in early dark phase. The higher antitumor effect of IFN-β was observed when specific binding of IFN receptor and DNA synthesis in tumor cells increased and the lower effect was observed when these levels decreased. The dosing time-dependent effect of IFN-β was supported by the time-dependent expression of transcription factor (STAT1) and cell proliferation inhibitor (p21WAF1) protein induced by IFN-β. There was a significant dosing time-dependent change in IFN-β concentration in tumor, with a higher level in early light phase and a lower level in early dark phase. However, IFN-β concentration was not high enough to elucidate the time-dependent effect of the drug because of low receptor occupancy at the concentration. The present results suggest that by choosing the most suitable dosing time for IFN-β, the efficacy of the drug can be increased in certain experimental and clinical situations.

Materials and Methods

Animals and cells: Male C57BL/6 mice (5 weeks old) were purchased from the Laboratory Animal Center, Faculty of Medicine, Kyushu University (Fukuoka, Japan). They were housed 8-10 per cage under standardized light-dark cycle conditions (lights on at 07:00, off at 19:00) at 24 ± 1 ℃ and 60 ± 10 % humidity with food and water available *ad libitum*. Their activity increases during the dark phase. Murine B16 melanoma cells (clone F1)(Dainippon Pharmaceutical Co. Ltd., Osaka, Japan) were maintained in vitro in Dulbecco's Modified Eagle's Medium (D-MEM) supplemented with 10 % heated-inactivated fetal bovine serum, 0.5 % kanamycin, 0.5 % penicillin and 0.5 % streptomycin at 37 ℃ in a humidified atmosphere with 5 % CO_2. Mice on day 7 after tumor cell implantation were used as tumor-bearing hosts. A 50 μl volume of 1.5×10^6 viable tumor cells was inoculated into the left hind footpads 7 days before drug treatment. Also, isolated tumor cells from tumor-bearing mice were cultured as described above.

Drugs: The lyophilized powder of natural human IFN-β (Feron®) (Toray Industries Inc., Tokyo, Japan) was dissolved in saline containing 0.1 % bovine serum albumin (BSA) and intratumorally (i.t.) injected (15 μl/10 g of body weight).

Experimental design: To determine the dose-response of the antitumor effect of IFN-β, groups of 6-7 tumor-bearing mice were injected intratumorally on days 0 - 6 (for 7 days) with 0.005, 0.05, 0.5 and 5 MIU/kg of IFN-β or saline at 09:00. The mice were monitored for day of death. Tumor volume was measured on day 12. To investigate the influence of dosing time on antitumor effect, groups of 6 - 12 tumor-bearing mice were injected intratumorally on days 0 - 6 with IFN-β (0.5 MIU/kg) or saline at 09:00 or 21:00. The mice were monitored for day of death. Tumor volume was measured every two days. In order to study the influence of IFN-β dosing time on STAT1 protein or p21WAF1 protein expression in implanted tumor cells, groups of 5 - 8 tumor-bearing mice were given an intratumoral injection of IFN-β (0.5 MIU/kg) or saline at 09:00 or 21:00. Their tumor masses were removed at 4 hr (for STAT1 protein) or 12 hr (for p21WAF1 protein) after IFN-β or saline injection. To investigate the specific binding of IFN-α to receptor on tumor cells, tumor masses were removed from

groups of 8 - 10 tumor-bearing mice at 09:00 or 21:00. In order to study the diurnal rhythm of IFNAR mRNA expression in implanted-tumor cells, tumor masses were removed from tumor-bearing mice at 09:00, 13:00, 17:00, 21:00, 01:00 or 05:00. To investigate the time-dependent change of STAT1 protein induced by IFN-β in implanted-tumor cells, tumor cells were isolated from tumor-bearing mice at 09:00 or 21:00. The cells were treated with IFN-β (0.01 MIU/ml) for 4 hr in vitro as described above. To study the influence of dosing time on IFN-β concentrations in tumor, groups of 44 - 51 tumor-bearing mice were given an intratumoral injection of IFN-β (0.5 MIU/kg) at 09:00 or 21:00. Tumor mass was removed at 0.05, 0.25, 0.5, 1, 2, 3 or 4 hr after IFN-β injection.

Determination of antitumor effect: Tumor volume was estimated using the formula: tumor volume (mg) = $4\pi xyz/3$, where 2x, 2y and 2z are the 3 perpendicular diameters of tumor. Relative tumor growth rate was expressed as the tumor volume change from the initiation of IFN-β or saline treatment. Survival time was estimated as the period from the initiation of treatment to death. Survival rate was calculated as the percent change for each group of 6 - 12 mice.

Western blot analysis: The removed tumor mass was placed into polypropylene tubes containing ice-cold hemolysis buffer (tris (hydroxymethyl) aminomethane(Tris)-buffered ammonium chloride) to remove erythrocytes. The isolated tumor mass was minced with scissors and centrifuged at $12000\times g$ for 5 min. The pellet was washed with ice-cold PBS and resuspended in ice-cold lysis buffer (120 mM NaCl, 100 mM NaF, 200 μM $Na_2V_2O_5$, 1 mM PMSF, 0.5 % NP-40, 0.001 % leupeptin, 50 mM Tris-HCl, pH 7.4). The pellet was homogenized with ice-cold lysis buffer and centrifuged at $12000\times g$ for 5 min. The tumor mass lysate containing 20-40 μg of total protein was mixed with an equal volume of 2×sample buffer (0.125 M Tris-HCl, pH 6.8, 10 % 2-mercaptoethanol, 4 % SDS, 10 % sucrose, 0.004 % bromophenol blue) and boiled at 95 ℃ for 5 min. The protein concentrations in tumor mass lysates were determined by Lowry's method (DC Protein Assay, Bio-Rad, California, US). The lysate sample was resolved by 8 % (for STAT1 protein) or 12 % (for p21WAF1) SDS-PAGE, transferred onto nitrocellulose membrane (Clear Blot Membrane-p, Atto Co., Tokyo,

Japan), and immunoblotted with the anti-STAT1 (STAT1 α or STAT1 β) mAb (Transduction Lab., Kentucky, USA) or the anti-p21WAF1 mAb (Oncogene Res. Prod., Cambridge, UK). Thereafter, the membrane was incubated with horseradish peroxidase-conjugated secondary antibody (mouse IgG). The blot was visualized with hydrogen peroxide in 3, 3', 5, 5'-tetramethylbenzidine and scanned with Deskscan II (Hewlett Packard Japan Co. Ltd., Tokyo, Japan). The band intensity was quantified by using NIH image program.

Specific IFN-α-binding assay: The iodination of IFN-β reduces its biological potency by < 30 % (Kushnaryov et al., 1985). Both IFN-α and -β cross-compete for the same receptor (Branca and Baglioni, 1981). Therefore, recombinant human IFN-α (Pepro Tech EC Ltd., London, England) was used as ligand to specific receptor of IFN-β. IFN-α was iodinated using a solid-phase lactoperoxidase kit (ICN Pharmaceuticals, Inc., Irvine, California, USA). The tumor cell suspension was prepared as described above and resuspended in ice-cold culture medium containing 0.25 % BSA, 0.1 % sodium azide, 10 μg/ml protamine sulfate and 2.5 mM $CaCl_2$. The binding assay was performed at 4 ℃ for 2 hr with a reaction mixture (total volume, 200 μl) containing 1 ng/ml [^{125}I]-IFN-α and 3×10^5 viable cells. After the incubation, 200 μl of heated-inactivated fetal bovine serum was added and the mixture centrifuged at 10000 rpm for 1 min. The supernatant was removed. Thereafter, the tube tip containing bound ligand was amputated and the radioactivity was measured using a gammer counter (ARC-360, Aloka Co., Mitaka, Tokyo, Japan). Nonspecific binding was evaluated in the presence of a 1500-fold excess of unlabeled IFN-α. Specific binding was calculated by subtracting nonspecific binding from total binding as follows: specific binding (%) = [(total binding - nonspecific binding) / total binding] × 100.

RNA extraction and RT-PCR. Total RNA was extracted from tumor masses by using TRIZOL® solution (BRL, Bethesda, MD, USA). The reverse transcription of RNA and cDNA amplification were perform with a one-step RT-PCR system (BRL). RT-PCR reactions were performed with IFNAR and glyceraldehyde-3-phosphate dehydrogenase (GAPDH) primers in a single tube. The following primers used: 5'-CATGGCTGGCTATATTGTTCC-3' and 5'-ATGGCTTGGGTTAAAGGTTTAC-3' for IFNAR (GenBank accession number; U06237), 5'-

GACCTCAACTACATGGTCTACA-3' and 5'-ACTCCACGACATACTCAGCAC-3' for GAPDH (GenBank accession number; M32599). The PCR product was electrophoresed through a 3 % agarose gel including 0.2 μg/ml ethidium bromide and the gel was photographed under UV light (302 nm). The amount of RT-PCR products of IFNAR mRNA was quantified using a NIH image analysis program and normalized against GAPDH.

Determination of IFN-β concentrations in tumor: The removed tumor mass was placed into ice-cold PBS containing 0.1 % BSA and leupeptin 10 μg/ml. The tumor mass in the buffer was homogenized and centrifuged at 12000$\times g$ for 5 min (Kubota Hematocrit KH-120A, Kubota, Tokyo, Japan). The supernatant was isolated and stored at -20 ℃ until assayed. The IFN-β concentrations in tumor were determined by an enzyme-linked-immunosorbent assay method (Human IFN-β ELISA kit , Toray Industries Inc., Tokyo, Japan). The coefficient of variation is less than 4 % and assay range is between 3 and 200 IU/ml. The recovery of IFN-β from tumor mass is more than 90 %. The protein concentrations in homogenate sample were determined by Lowry's method.

NONMEM analysis: The population pharmacokinetic parameters were calculated on an HP-9000 series 700 (Yokogawa-Hewlett Packard Ltd., Tokyo, Japan) with the NONMEM program (version IV, level 1.1), following the two-compartment model (the PREDPP program, subroutines ADVAN3 and TRANS1). Bayesian estimates of individual pharmacokinetic parameters were obtained with the posthoc method of the NONMEM program. The statistical moment parameters such as area under the curve (AUC) and mean residence time (MRT) were calculated by using the estimated individual pharmacokinetic parameters.

Statistical analysis: The values were validated for each phase among six different sampling times by analysis of variance (ANOVA). ANOVA and Tukey's test were applied for the multiple comparison. Student's t-test was used for two independent groups. Survival curves were compared with the Log-Rank test. The 5 % level of probability was considered to be significant.

Results

Dose-response effects of IFN-β on tumor growth or survival: The effects of various dosages (0.005, 0.05, 0.5 and 5 MIU/kg, i.t.) of IFN-β on tumor growth or survival time in tumor-bearing mice injected with the drug at the same circadian phase (09:00) are shown in Table 1. Tumor growth on day 12 after initiation of IFN-β (0.5 or 5 MIU/kg) treatment was significantly suppressed compared with that in the control group given saline ($P<0.05$). Also, the survival time after initiation of IFN-β (0.5 or 5 MIU/kg) treatment was significantly prolonged compared with that in the control group ($P<0.05$). However, the tumor growth and survival time did not differ significantly between tumor-bearing mice injected with IFN-β (0.005 or 0.05 MIU/kg) and with saline.

Influence of dosing time on tumor growth or survival: All tumor-bearing mice injected with saline at 09:00 or 21:00 died between day 14 and day 22. No significant effect of dosing time was observed for survival after saline injection (data not shown). Also, no dosing time-dependent change in the rate of tumor growth was observed on day 12 after initiation of saline injection (data not shown). Therefore, a mean value between 09:00 and 21:00 is shown as the control in Fig.1. The tumor growth in tumor-bearing mice on day 9 or day 12 after initiation of IFN-β (0.5 MIU/kg) treatment at 09:00 or 21:00 was significantly suppressed when compared with that in control mice given saline ($P<0.05$, respectively, Fig.1). The tumor growth in tumor-bearing mice on day 12 after initiation of IFN-β injection at 09:00 was significantly reduced relative to that in mice injected with IFN-β at 21:00 ($P<0.05$). Also, the survival time after IFN-β injection at 09:00 was significantly longer than that after saline injection ($P<0.05$, Fig.1). However, the survival time after IFN-β injection at 21:00 was not significantly different from that after saline injection or IFN-β injection at 09:00.

Influence of IFN-β dosing time on STAT1 protein level in tumor masses: As shown in Fig. 2, the STAT1 α or STAT1 β protein level at 4 hr after a single injection of IFN-β (0.5 MIU/kg) at 09:00 was significantly higher when compared with that after saline injection at 09:00 (STAT1 α; $P<0.01$, STAT1 β; $P<0.05$). However, the protein level at 4 hr after IFN-β injection at 21:00 was not significantly different from that after saline injection at 21:00.

Influence of IFN-β dosing time on p21WAF1 protein level in tumor masses: As shown in Fig. 3, the p21WAF1 protein level at 12 hr after a single injection of IFN-β (0.5 MIU/kg) at 09:00 or 21:00 was significantly higher when compared with that after saline injection at the corresponding dosing time ($P<0.01$, respectively). Furthermore, it was significantly higher in tumor-bearing mice injected with IFN-β at 09:00 than at 21:00 ($P<0.05$).

Diurnal rhythm of specific IFN-α-binding and IFNAR mRNA expression in isolated tumor cells: The specific binding of IFN-α to receptor was significantly greater in tumor cells prepared at 09:00 than in tumor cells prepared at 21:00 ($P<0.05$, Fig.4). Also, the IFNAR mRNA level in tumor cells from tumor-bearing mice showed a significant diurnal rhythm dependence ($P<0.05$, ANOVA, Fig.5). The mRNA level was higher at 09:00 and 13:00 and lowest at 21:00.

Time-dependent change of STAT1 protein induction by IFN-β in isolated tumor cells: The time-dependent change of STAT1 protein expression induced by IFN-β was demonstrated for tumor cells prepared from tumor-bearing mice at 09:00 or 21:00 (Fig.6). The STAT1 protein induction by IFN-β was significantly more potent in tumor cells obtained at 09:00 than at 21:00 ($P<0.05$). The STAT1 protein level in tumor cells prepared at 09:00 was significantly higher in the treatment with IFN-β than without IFN-β ($P<0.01$). However, the STAT1 protein level in tumor cells prepared at 21:00 was not significantly different between both treatments.

Influence of dosing time on IFN-β pharmacokinetics: The time course of the change in IFN-β concentration in tumor after a single injection of IFN-β (0.5 MIU/kg) decreased in a biexponential fashion. The concentrations in tumor at 3 or 4 hr after IFN-β injection at 09:00 were significantly higher than those after the drug injection at 21:00 ($P<0.01$, Fig.7). Table 2 shows the pharmacokinetic parameters after IFN-β injection. The analysis was conducted by using 95 tumor concentrations obtained from 95 mice. The final model equations estimated for all data were as follows: total body clearance (CL) (mg protein/hr) = 24.9×1.22^{DT}, central volume of distribution (Vc) (mg protein) = 12.3, k12 (1/hr) = 2.04, k21 (1/hr) = 2.57, where

CL, Vc, k12 and k21 are total clearance, central volume of distribution, distribution rate constant from central to peripheral compartment, and distribution rate constant from peripheral to central compartment, respectively. DT represents dosing time: DT = 0 if injection at 09:00; DT = 1 if injection at 21:00. Using the population parameters, individual pharmacokinetic parameters was calculated based on Bayesian estimate and then AUC and MRT were derived from them. CL was significantly larger in mice injected with IFN-β at 21:00 than at 09:00 ($P<0.01$). AUC, MRT, $t_{1/2}\alpha$ and $t_{1/2}\beta$ were significantly larger in mice injected with IFN-β at 09:00 than at 21:00 ($P<0.01$, respectively).

Discussion

IFNs have a capacity to inhibit the proliferation of various tumor cell lines (Ida et al., 1982; Gomi et al., 1983, 1986). And IFN-β is more potent in melanoma cell lines than other tumor cell lines (Ida et al., 1982; Gomi et al., 1983). In the present study, the growth of B16 melanoma implanted in mice was inhibited by IFN-β in a dose-dependent manner. Furthermore, the antitumor effect after IFN-β injection was significantly more potent in tumor-bearing mice injected with the drug at 09:00 than at 21:00. This result confirms a previous chronopharmacological finding on the antitumor effect of IFN-α (Koren et al., 1993). In general, the rhythmic change of drug response is caused by that of pharmacokinetic factors such as drug concentration at the site of action and/or pharmacodynamic factors such as receptor sensitivity to drug.

IFNs mediate biological effects through activation of the JAK-STAT signaling pathway (Darnell et al., 1994). IFN-inducible STAT1 (STAT1α or STAT1β) and STAT2 associate with a 48 kDa protein to form the transcription factor, IFN-stimulated gene factor-3 (ISGF3) complex (Qureshi et al., 1995). This complex binds to the IFN-stimulated response element (ISRE) and modulates various genes (Levy et al., 1989). Also, the STAT1 protein-activating effect of IFN-α is differentially influenced by the stage of the cell cycle (Kumar et al, 1994). In the present study, the STAT1 protein level in tumor cells was significantly higher after injection of IFN-β than saline at 09:00. This result is consistent with the time-dependent change in the specific binding of IFN-α. Thus, the dosing time-dependent change in the STAT1 protein-increasing effect of IFN-β may be caused by that in the specific binding of IFN-α to receptor on tumor cells.

The p21WAF1 protein level in tumor cells after IFN-β injection at 09:00 was significantly higher than that after saline injection at 09:00 or the drug injection at 21:00. This result corresponded to the dosing time-dependent change in the STAT1 protein-enhancing effect of IFN-β. The progression of the cell cycle is regulated by a number of essential proteins that stimulate or inhibit transition between the different phases of the cycle. The cdks facilitate the restriction point transition in cell cycle progression (Hunter and Pine, 1994). In particular, cdk2 and cdk4 regulate entry from the G1 phase into the S phase. IFN-α inhibits cell proliferation

through the upregulation of cdk-inhibitor p21WAF1 which inhibits the cdk2 and cdk4 activity (Sangfelt et al, 1997; Mandal et al, 1998). On the other hand, the activated STAT1 protein specifically recognizes the conserved STAT-responsive elements in the promoter of the gene encoding p21WAF1 and regulates the induction of p21WAF1 mRNA (Chin et al., 1996). IFN-α or -γ does not inhibit the proliferation of tumor cells lacking STAT1 expression (Thornton et al., 1996; Sun et al., 1998). Thus, the dosing time-dependent change in the p21WAF1 protein-increasing effect of IFN-β seems to be caused by that in the STAT1 expression and influence the antitumor effect of IFN-β in a dosing time-dependent manner.

While both IFN-α and -β elicit antitumor and antiviral activity by binding to the same specific receptor on the cell surface, IFN-γ binds to a distinct receptor (Branca and Baglioni, 1981; Zoon and Arnheiter, 1984). On the other hand, the specific binding of the IFN-α receptor in chronic myelogenous leukemia cells is upregulated by synchronizing the cells mainly in early S phase by hydroxyurea treatment (Tamura et al., 1997). The increase of binding is caused by an increase in the number of binding sites with a constant receptor affinity. The proportion of tumor cells in S phase showed a significant diurnal rhythm with higher levels in the late dark phase and the early light phase and lower ones in the late light phase (data not shown). Namely, more specific binding of IFN-α was observed when the proportion of tumor cells in S phase increased and less binding when it decreased. These results suggest that the time-dependent change of IFN-β antitumor effect is related to that of the sensitivity, particularly at the receptor level, of tumor cells to IFN-β.

IFN-β concentrations in tumor were significantly higher after IFN-β injection at 09:00 than at 21:00. A significant dosing time-dependent difference was also demonstrated for the pharmacokinetic parameters of IFN-β, which showed higher CL for injection at 21:00 than at 09:00. The rhythmicity of CL seems to be closely related to that of IFN-β concentrations in tumor. The drug clearance is determined by intrinsic clearance or blood flow in metabolic or excretive organs. In this study, the predominant pathway of IFN-β elimination is via the tumor cells, since the drug was directly administered into tumor tissue. IFN-α is internalized via receptor-mediated endocytosis and catabolized intracellulary by lysosomal proteinases in metabolic tissue (Bocci et al., 1983). Moreover, the receptor-mediated uptake contributes to the body clearance of cytokine such as granulocyte colony-stimulating factor (Kuwabara et al.,

1994) and erythropoietin (Kato et al., 1997). However, the higher CL of IFN-β was observed when the specific binding of IFN-α to receptor decreased. Also, the diurnal rhythm of blood flow in eliminative organs partially influences the time-dependent change of drug pharmacokinetics (Labrecque et al., 1988). The blood flow rate in the tumor tissue is significantly higher during the active phase than the rest phase in rats (Hori et al., 1995). Therefore, the dosing time-dependent change in IFN-β concentration in tumor may be partially explained by the diurnal rhythm of blood flow in tumor mass. The dosing time-dependent difference in antitumor effect of IFN-β was consistent with that in MRT as well as AUC. A longer exposure to an effective concentration may be important to obtain an efficient antitumor effect of IFN-β, because IFN-β inhibits the proliferation of various tumor cell lines in not only a concentration-dependent but also a time-dependent manner in vitro (Yamada and Shimoyama, 1983; Wong et al, 1989). However, the IFN-β concentrations in tumor at 3 or 4 hr after the drug injection was low, and the receptor occupancy predicted from the IFN-β concentrations in tumor and apparent affinity of IFN-α to its receptor (See Table 3) is only 2 - 3 %. Also, in the dose-response effect of IFN-β on tumor growth, the degree of antitumor effect observed at 21:00 with 0.5 MIU/kg of IFN-β was approximately agreed with that observed at 09:00 with a dosage 0.1 MIU/kg of IFN-β (data not shown). The observed difference of AUC or MRT by IFN-β dosing time was only 1.2 times. Thus, the diurnal rhythm of IFNAR expression in tumor rather than IFN-β pharmacokinetics seems to be closely related to that of the antitumor effect induced by IFN-β.

The present study suggests that the dosing time-dependent change in the antitumor activity of IFN-β is caused by that in the sensitivity of tumor cells to IFN-β. Therefore, the choice of dosing time based on the diurnal rhythm in IFNAR expression on tumor cells may help us to establish a rational chronotherapeutic strategy, increasing the antitumor activity of the drug in certain clinical situations.

Table 1 Dose-response effects of IFN-β on tumor growth or survival time

IFN-β dose (MIU/kg, i.t.)	Relative tumor growth rate	Survival time (days)
0	21.732 ± 3.283	18.333 ± 0.989
0.005	20.156 ± 1.291	18.714 ± 0.680
0.05	15.308 ± 1.679	20.667 ± 2.155
0.5	8.637 ± 0.961*	27.143 ± 2.492*
5	6.843 ± 0.572*	29.143 ± 2.327*

Drug injection is performed at 09:00. Each value is the mean with S.E. of 6-7 mice.
*P<0.05 when compared with the saline (0 MIU/kg) group using Tukey's test.

Table 2 Influence of dosing time on pharmacokinetic parameters after IFN-β (0.5 MIU/kg, i.t.) injection at 09:00 or 21:00

Pharmacokinetic parameters		Time of drug injection (clock hours) 09:00	21:00	Student's t-test
CL	(g protein/hr/kg)	1.156 ± 0.015	1.436 ± 0.019	P<0.01
Vc	(g protein/kg)	0.574 ± 0.006	0.587 ± 0.006	N.S.
t1/2 α	($\times 10^{-1}$ hr)	0.587 ± 0.004	0.503 ± 0.004	P<0.01
t1/2 β	($\times 10^{-1}$ hr)	7.677 ± 0.059	6.638 ± 0.054	P<0.01
AUC	(IU · hr/mg protein)	435.891 ± 5.298	350.641 ± 4.556	P<0.01
MRT	(hr)	0.894 ± 0.009	0.735 ± 0.008	P<0.01

Each value is the mean with S.E. of 44-51 mice.

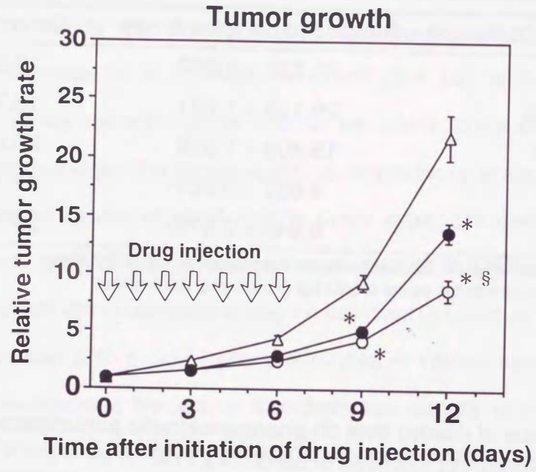

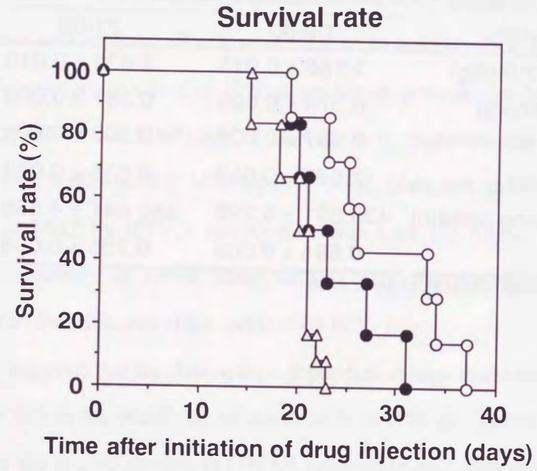

Fig. 1 Influence of dosing time on tumor growth or survival rate (%) after IFN-β (0.5 MIU/kg, i.t.)(○; 09:00, ●; 21:00) or saline (△; 09:00 or 21:00) injection on days 0-6 (for 7 days). Each value is the mean with S.E. of 6-12 mice. *P<0.05 when compared with the corresponding saline group, §P<0.05 when compared between the two dosing times using Tukey's test. Survival rate after IFN-β treatment at 09:00 was significantly greater than that after saline treatment (P<0.05 using Log-Rank test).

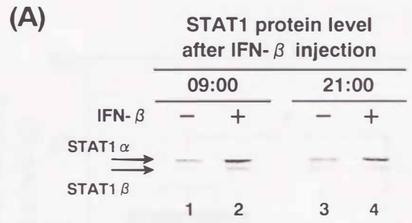

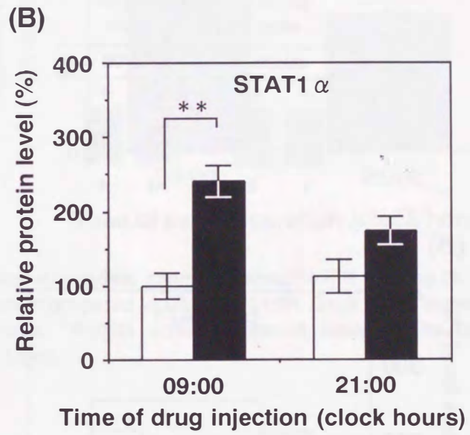

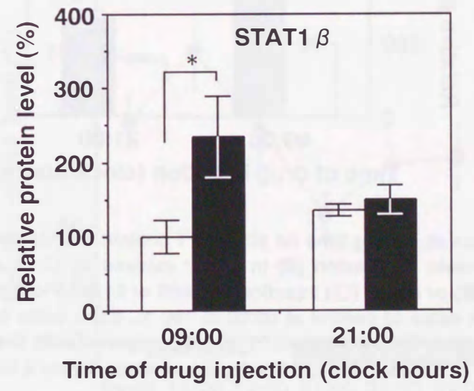

Fig. 2 Influence of dosing time on STAT1 (STAT1α or STAT1β) protein expression (A) or relative STAT1 protein expression (B) in tumor masses at 4 hr after IFN-β (0.5 MIU/kg, i.t.)(■) or saline (□) injection at 09:00 or 21:00. Plots of band intensity set the mean value of control at 09:00 at 100 %. Each value is the mean with S.E. of 5-6 mice. *P<0.05, **P<0.01 when compared with the corresponding saline group using Tukey's test.

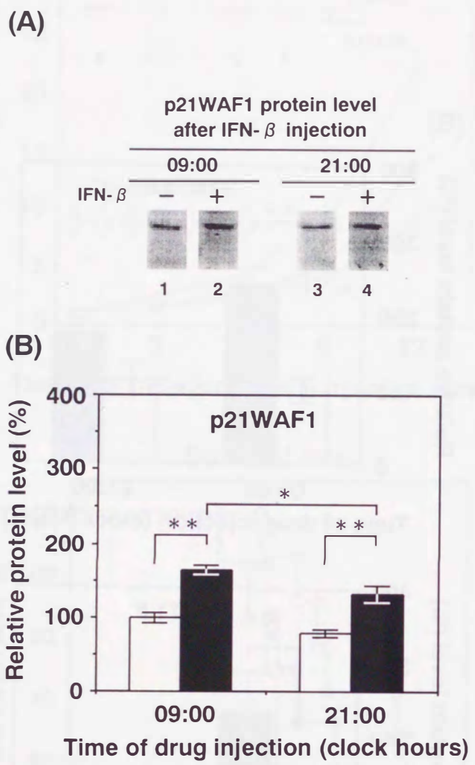

Fig.3 Influence of dosing time on p21WAF1 protein expression (A) or relative p21WAF1 protein expression (B) in tumor masses at 12 hr after IFN-β (0.5 MIU/kg, i.t.)(■) or saline (□) injection at 09:00 or 21:00. Plots of band intensity set the mean value of control at 09:00 at 100 %. Each value is the mean with S.E. of 7-8 mice. *P<0.05, **P<0.01 when compared with the corresponding saline group or between the two dosing times using Tukey's test.

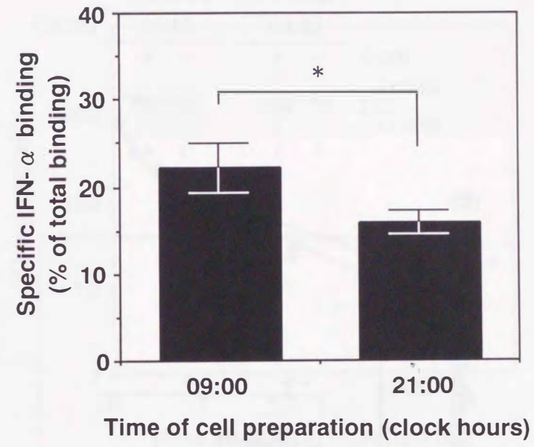

Fig. 4 Time-dependent change in specific IFN binding (% of total binding) to tumor cells prepared at 09:00 or 21:00. Each value is the mean with S.E. of 8-10 mice. *P<0.05 when compared between the two times using Student's t-test.

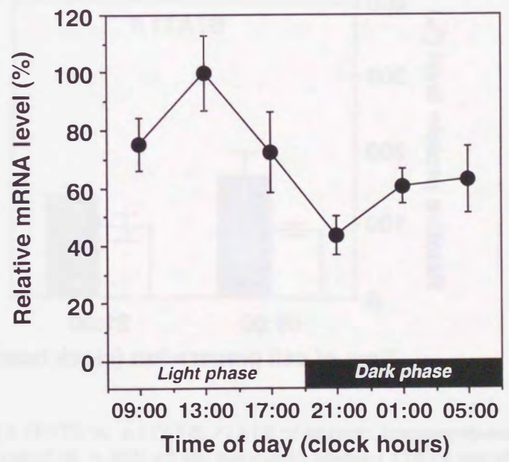

Fig.5 Diurnal rhythm of IFNAR mRNA level (%) in tumor cells prepared at six different times. Relative mRNA level sets the mean value at 13:00 at 100 %. Each value is the mean with S.E. of 6 mice. IFNAR mRNA level showed a significant diurnal rhythm (P<0.05, ANOVA).

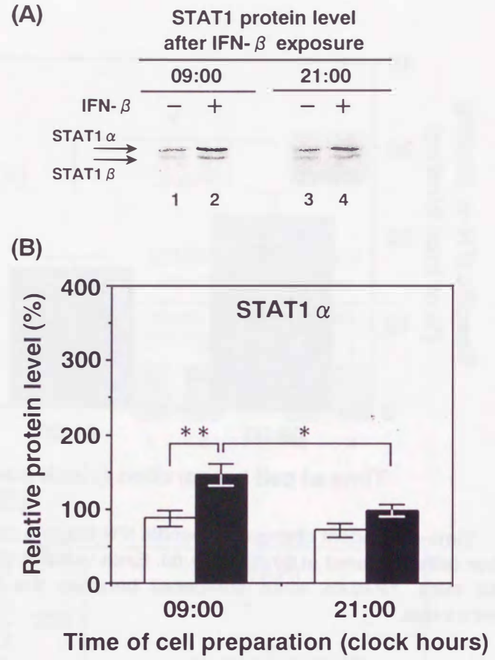

Fig.6 Time-dependent change in STAT1 (STAT1 α or STAT1 β) protein induction (A) or relative STAT1 protein induction (B) by IFN-β in tumor cells prepared at 09:00 or 21:00 from tumor-bearing mice. Isolated tumor cells were cultured with (■) or without (□) IFN-β (0.01 MIU/mL). Relative protein level sets the mean value of control at 09:00 at 100 %. Each value is the mean with S.E. of 5 mice. *P<0.05, **P<0.01 when compared between two groups using Tukey's test.

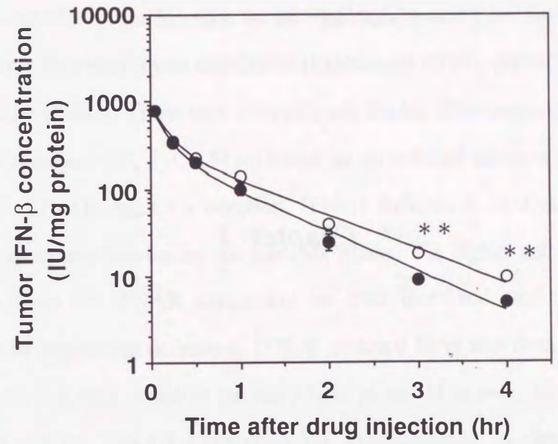

Fig. 7 Influence of dosing time on IFN-β concentrations in tumor after IFN-β (0.5 MIU/kg, i.t.) injection at 09:00 (○) or 21:00 (●). Each value is the mean with S.E. of 5-11 mice. **P<0.01 when compared between the two dosing times using Student's t-test.

Chapter 1

Influence of IFN-β Dosing Time on Its Pharmacological Effects in Mice

1-2 Influence of IFN-β Dosing Time on Antiviral Effect in Mice

Abstract

The influence of IFN-β dosing time on antiviral activity and fever was investigated in ICR male mice under a light-dark cycle conditions (lights on at 07:00, off at 19:00) with food and water available *ad libitum*. There was a significant dosing time-dependent change in 2', 5'-oligoadenylate synthetase (2', 5'-OAS) activities, as an index of antiviral activity, in liver at 12 hr after IFN-β (15 MIU/kg, i.v.) injection. IFN-β-induced 2', 5'-OAS activity were more potent after the drug injection during the late dark phase. The higher antiviral effect of IFN-β was observed when the IFNAR expression on liver increased, and the lower effect was observed when its expression decreased. IFN-β-induced fever was more serious after IFN-β injection from the late dark phase to the early light phase. However, there was no significant diurnal rhythm for the IFNAR expression on hypothalamus. A significant dosing time-dependent change was demonstrated for plasma IFN-β concentrations, which showed a higher level during light phase and a lower level during the dark phase. The dosing time-dependent change of plasma IFN-β concentrations was not associated with that of antiviral effect or fever induced by IFN-β. These results suggest that a setting of the most suitable dosing time of IFN-β, associated with the diurnal rhythm of IFNAR expression on liver, may be important to increase effectively the antiviral activity of the drug in experimental and clinical situations.

Materials and Methods

Animals: Male ICR mice (5 weeks old) were purchased from the Charles River Japan Inc. (Kanagawa, Japan). They were housed 8 - 10 per cage under standardized light-dark cycle conditions (lights on at 07:00, off at 19:00) at 24 ± 1 ℃ and 60 ± 10 % humidity with food and water available *ad libitum*.

Drugs: The lyophilized powder of natural human IFN-β (Feron®) (Toray Industries Inc., Tokyo, Japan) was dissolved in saline and intravenously (i.v.) injected (0.05 ml/kg of body weight).

Experimental design: To investigate the influence of IFN-β dosing time on 2', 5'-OAS mRNA level and activity, groups of 7 - 8 mice were injected with IFN-β (15 MIU/kg, i.v.) or saline at once of six times: 09:00, 13:00, 17:00, 21:00, 01:00 or 05:00. The liver samples were quickly removed at 4 hr (for mRNA) or 12 hr (for activity) after IFN-β (15 MIU/kg, i.v.) or saline injection and placed into ice-cold tubes. To examine the influence of IFN-β dosing time on rectal temperature, groups of 6 mice were injected with IFN-β (15 MIU/kg, i.v.) or saline at each of the six times outlined above. Rectal temperatures were measured at 0.5 hr after IFN-β or saline injection. In order to study the diurnal rhythm of IFNAR mRNA expression in liver, hypothalamus or lymphocytes, each tissues were removed from groups of 5 - 6 mice at each of the six times outlined above. To investigate the time-dependent change in specific binding of IFN-α to IFNAR on lymphocytes, lymphocytes were obtained from groups of 5 mice at 17:00 or 05:00. To examine the diurnal rhythm of plasma IFN-β concentration at 2.5 hr after IFN-β injection, groups of 5 - 6 mice were injected with IFN-β (15 MIU/kg, i.v.) or saline at each of the six times outlined above. Also, to determine the influence of IFN-β dosing time on time course of plasma IFN-β concentrations, groups of 5 - 6 mice were given an intravenous injection of IFN-β (15 MIU/kg) at 09:00 or 21:00. Blood samples were collected at 0.167, 0.5, 1, 1.5 or 3 hr after IFN-β injection.

RNA extraction and RT-PCR. Total RNA was extracted from liver, hypothalamus or lymphocytes by using TRIZOL® solution (BRL, Bethesda, MD, USA). The reverse transcription of RNA and cDNA amplification were perform with a one-step RT-PCR system (BRL). RT-PCR reactions were performed with 2', 5'-OAS, IFNAR and glyceraldehyde-3-phosphate dehydrogenase (GAPDH) primers in a single tube. The following primers used: 5'-GCAAGCCTGATCCCAGAATCT-3' and 5'-TAGCCACACATCAGCCTCTTCA-3' for 2', 5'-OAS (GenBank accession number; X04958), 5'-CATGGCTGGCTATATTGTTCC-3' and 5'-ATGGCTTGGGTTAAAGGTTTAC-3' for IFNAR (GenBank accession number; U06237), 5'-GACCTCAACTACATGGTCTACA-3' and 5'-ACTCCACGACATACTCAGCAC-3' for GAPDH (GenBank accession number; M32599). The PCR product was electrophoresed through a 3 % agarose gel including 0.2 μg/ml ethidium bromide and the gel was photographed under UV light (302 nm). The amount of RT-PCR products of 2', 5'-OAS or IFNAR mRNA was quantified using a NIH image analysis program and normalized against GAPDH.

Determination of 2', 5'-OAS activity. Liver was perfused with Phosphate-buffered saline and removed, placed into ice-cold tube containing modified lysis buffer (10 mM HEPES-KOH / 50 mM KCl / 3 mM $Mg(OAc)_2$ / 0.3 mM EDTA / 10 % glycerol / 0.01 % NaN_3 / 0.5 % Triton-100 / 100 μM PMSF / 7 mM 2-mercaptoethanol, pH 7.5) (Sokawa et al, 1994). The liver in the buffer was homogenized and centrifuged at 9000$\times g$ for 20 min at 4 ℃. The supernatant was isolated and stored at - 20 ℃. The protein concentrations in the liver homogenate sample were determine by Lowry's method. The liver 2', 5'-OAS activities were determined by radioimmunoassay (2-5 A kit, Eiken, Tokyo, Japan). The 2', 5'-OAS activities were expressed as 2', 5'-oligoadenylate fmol per protein concentration.

Determination of rectal temperature. Rectal temperature was measured by a digital thermometer (Digital Thermometer TD-300, Shibaura Electronics, Tokyo, Japan). A lubricated thermocouple was inserted 1.5 cm into the rectum of mice. Rectal temperature was measured at least every 30 min to avoid hyperthermia caused by continuous handling stress (Briese et al, 1991). Percent change of rectal temperature (%) from basal level was calculated as follows: % = ([rectal temperature after IFN-β injection – rectal temperature before IFN-β injection] / [rectal temperature before IFN-β injection]) × 100.

Lymphocyte isolation. Spleen samples were homogenized to obtain a single-cell suspensions including lymphocytes. Then the splenic lymphocytes were isolated by a density-gradient separation (Lympholyte-M®, Cosmo Bio, Tokyo, Japan). The isolated lymphocytes were suspended in Tris-buffered ammonium chloride to remove erythrocytes and were washed twice in PBS.

Specific IFN-α binding assay. The iodination of IFN-β reduces its biological potency by < 30 % (Kushnaryov et al., 1985). Both IFN-α and -β cross-compete for the same receptor (Novick et al, 1994). Therefore, recombinant human IFN-α (Pepro Tech EC Ltd., London, England) was used as ligand to specific receptor of IFN-β. IFN-α was iodinated using a solid-phase lactoperoxidase kit (ICN Pharmaceuticals, Inc., Irvine, California, USA). The splenic lymphocytes were isolated as described above and resuspended in ice-cold RPMI 1640 medium containing 0.25 % BSA, 0.1 % sodium azide, 10 μg/ml protamine sulfate, 2.5 mM $CaCl_2$ and the indicated concentrations of [^{125}I-IFN-α]. The binding assay was performed at 4 ℃ for 2 hr with reaction mixture (a total volume 200 μl) containing various concentrations of [^{125}I-IFN-α] and 1×10^6 cells viable cells. After incubation, the reaction mixture was layered over 200 μl of heated-inactivated fetal bovine serum and centrifuged at 10000 rpm for 1 min. The supernatant was removed. Thereafter, the tube tip containing bound ligand was amputated and the radioactivity was measured using a gammer counter (ARC-360, Aloka Co., Mitaka, Tokyo, Japan). Nonspecific binding was evaluated in the presence of at least 250-fold excess of unlabeled IFN-α. Specific binding was defined as nonspecific binding subtracted from total binding. The data were plotted according to the method of Scatchard (Scatchard, 1949). A molecular weight of 20,000 was assumed for the calculation of the receptor number per cell and the dissociation constant (Kd).

Determination of plasma IFN-β concentrations. Blood samples were collected by orbital sinus and plasma samples were obtained after centrifugation at 3000 rpm for 3 min (Kubota Hematocrit KH-120A, Kubota, Tokyo, Japan) and stored at - 20 ℃ until assayed. Plasma IFN-β concentrations were determined by enzyme-linked-immunosorbent assay method (Human IFN-β ELISA kit, Toray Co., Tokyo, Japan).

Pharmacokinetic analysis: Pharmacokinetic parameters were calculated by the nonlinear least-squares method, following the two-compartment model: total body clearance (CL), central volume of distribution (Vc), distribution rate constant from central to peripheral compartment (k_{12}) and distribution rate constant from peripheral to central compartment (k_{21}).

Statistical analysis. Analysis of variance (ANOVA) and Tukey's test were applied for the multiple comparison. Student's t-test was used for two independent groups. The 5 % level of probability was considered to be significant.

Results

Influence of IFN-β dosing time on liver 2', 5'-OAS mRNA expression and activity: The 2', 5'-OAS mRNA level in liver at 4 hr after IFN-β (15 MIU/kg, i.v.) injection was significantly higher in mice treated with the drug at 01:00 or 5:00 ($P<0.01$, Fig.8). However, the 2', 5'-OAS mRNA in liver was not detected at 4 hr after saline injection at any dosing times. On the other hand, the 2', 5'-OAS activity in liver at 12 hr after IFN-β injection at 05:00 or 17:00 was significantly higher when compared with that after saline injection ($P<0.01$, respectively, Fig.9). Furthermore, the 2', 5'-OAS activity in liver at 12 hr after IFN-β injection at 05:00 was significantly higher than that after IFN-β injection at 17:00 ($P<0.05$). No dosing time-dependent change was observed for 2', 5'-OAS activity in liver at 12 hr after saline injection.

Influence of IFN-β dosing time on rectal temperature: The rectal temperature showed a significant diurnal rhythm with a lower level during the light phase and a higher level during the dark phase ($P<0.01$, ANOVA, Fig.10). The percent change of rectal temperature at 0.5 hr after IFN-β (15 MIU/kg, i.v.) injection at 09:00, 13:00 or 05:00 was significantly higher than that after saline injection at the corresponding dosing time ($P<0.01$, respectively, Fig.11). However, fever was not induced by IFN-β injection at 17:00, 21:00 or 01:00.

Diurnal rhythm of IFNAR expression in liver, hypothalamus and lymphocyte: The IFNAR mRNA level in liver and lymphocyte showed a significant diurnal rhythm ($P<0.01$, respectively, ANOVA, Fig.12). The IFNAR mRNA level in liver was higher during the late dark phase and lower during the late light phase. The IFNAR mRNA level in lymphocytes was higher during the late dark phase and the early light phase, and lower during the late light phase and the early dark phase. However, no significant diurnal rhythm was observed in the IFNAR mRNA level of hypothalamus (Fig.12). Furthermore, the number of IFNAR per cell of lymphocytes, calculated from the intercept of the Scatchard plot on the abscissa, was significantly larger in cells prepared at 05:00 than at 17:00 ($P<0.01$, Table 3). The apparent Kd showed no significant difference between cells prepared at 05:00 and 17:00.

Influence of dosing time on IFN-β pharmacokinetics: The plasma IFN-β concentrations at 2.5 hr after IFN-β (15 MIU/kg, i.v.) injection showed a significant diurnal rhythm with higher levels during the light phase and lower during the dark phase ($P<0.01$, ANOVA, Fig.13). The influence of dosing time on time course of plasma IFN-β concentrations after IFN-β injection is shown in Table 4. The time course of plasma IFN-β concentrations after IFN-β injection decreased in biexponential fashion. Plasma IFN-β concentrations at 1.5 and 3 hr after IFN-β injection at 09:00 were significantly higher when compared with those after the drug injection at 21:00 ($P<0.05$, respectively). Table 5 showed the pharmacokinetic parameters after IFN-β injection. CL was significantly higher in mice injected with IFN-β at 21:00 than at 09:00 ($P<0.05$).

Discussion

Antiviral efficacy of IFN is mediated through production of 2', 5'-OAS activated by double-stranded RNA (Lengyel, 1982). 2', 5'-OAS activates a latent ribonuclease, can cleave single-stranded RNA, and impairs replication of various virus (Kumar et al., 1988, Diaz-Guerra et al., 1997). In this study, the 2', 5'-OAS mRNA induction and its activity in liver after IFN-β injection were significantly more potent in mice injected with the drug during the late dark phase. This result was supported by a previous chronopharmacological finding of IFN-α (Koyanagi et al., 1997).

IFN elicits antiviral activity by binding to the specific receptor on the cell surface (Zoon and Arnheiter, 1984). In IFNAR-deficient cell lines, IFN-α and -β fail to induce 2', 5'-OAS activity and protect against viral infection (Hwang et al., 1995). Furthermore, the level of IFNAR expression in liver is closely related to the efficacy of IFN-α therapy in patients with chronic hepatitis C (Fukuda et al., 1997; Yatsuhashi et al., 1999). In the present study, the level of IFNAR mRNA in liver showed a significant diurnal rhythm with a higher level during the late dark phase and lower level during the late light phase. In addition, we examined the binding assay for IFNAR by using the lymphocytes, because the homogenization and processing of membranes for binding alter the binding kinetics of the receptor (Davis et al., 1979). The number of IFNAR per cells was significantly larger in cells obtained at 05:00 than at 17:00. These results indicate that the rhythmic change of IFNAR mRNA level is associated with that of the the number of IFNAR. Moreover, the diurnal rhythm of IFNAR mRNA level in liver was consistent with the dosing time-dependent change of 2', 5'-OAS mRNA induction and its activation in liver by IFN-β. On the other hand, the plasma IFN-β concentrations at 2.5 hr after IFN-β injection was higher during the light phase and lower during the dark phase. Namely, the rhythmicity of plasma IFN-β concentration was out of phase with the dosing time-dependent change of 2', 5'-OAS activation induced by IFN-β. Therefore, the time-dependency in 2', 5'-OAS activation of IFN-β seems to be due to not the rhythmicity of IFN-β pharmacokinetics but that of IFNAR expression.

The change of rectal temperature at 0.5 hr after IFN-β injection during the late dark phase and the early light phase was significantly higher than that after saline injection at the corresponding dosing time. However, no significant dosing time-dependence was observed for IFN-β concentrations at 0.5 hr after IFN-β injection. The IFNAR mRNA expression in hypothalamus showed some rhythmic pattern but not significant rhythm at present. IFN-α elicits fever through the direct action on preoptic-anterior hypothalamic thermosensitive neurons (Nakashima et al., 1988). IFN-α-induced fever is mediated by prostagrandin E2 (PGE_2) production and/or opioid receptor mechanism in hypothalamus (Nakashima et al., 1995). However, IFN-β is a lack of binding capacity to opioid receptors in the brain (Blalock and Smith, 1981). The dosing time-dependent difference of fever induced by IFN-α is caused by that of PGE_2 production induced by the drug (Koyanagi et al., 1997; Ohdo et al., 1997a). The fever induced by IFN-β was completely inhibited by indomethacin (10 mg/kg, i.p.) pretreatment, although the dosage of indomethacin had no effect on normal rectal temperature (data not shown). Cyclooxygenase-2 (COX-2) plays a major role in the rapid production of PGE_2 and fever induced by IL-1β (Cao et al., 1996). Glucocorticoid inhibits the elevation of COX-2 mRNA as well as PGE_2 formation induced by IL-1β (Masferrer et al., 1994; Yucel-Lindberg et al., 1995). In rodents, plasma glucocorticoid hormone such as corticosterone shows a diurnal rhythmicity with elevation during late light phase and early dark phase. In this study, the serious fever induced by IFN-β was observed when plasma glucocorticoid level was lower. Thus, the time-dependency in fever induced IFN-β may be due to the rhythmicity of plasma glucocorticoid level.

IFN-β concentrations at 1.5 or 3 hr after IFN-β injection at 09:00 were significantly higher than those after IFN-β injection at 21:00. A significant dosing time-dependent difference was also demonstrated for the pharmacokinetic parameter of IFN-β, which showed higher CL for injection at 21:00 than for injection at 09:00. The rhythmicity of CL seems to contribute to that of plasma IFN-β concentrations. The drug clearance is determined by blood flow rate or intrinsic clearance in metabolic or excretive organs. The predominant pathway of IFN-β elimination is the liver (Wills, 1990). IFN-α is internalized via receptor-mediated endocytosis and catabolized intracellulary by lysosomal proteinases in metabolic tissue (Bocci et al., 1983). The receptor-mediated saturable clearance of granulocyte colony-stimulating factor

mainly contributes to the its total clearance at lower doses (Kuwabara et al., 1994). However, CL was significantly higher in mice injected with IFN-β at 21:00 than at 09:00, although the IFNAR mRNA level in liver was higher at 09:00 than at 21:00. Also, the blood flow in liver shows significant diurnal rhythm with higher level during the dark phase and lower during the light phase (Labrecque et al., 1988). The rhythmicity in CL or concentrations of IFN-β at 2.5 hr after IFN-β injection in our study was consistent with that in blood flow to liver. Thus, the diurnal rhythm of blood flow may contribute to the dosing time-dependent change of IFN-β pharmacokinetics.

In conclusion, I have shown here the dosing time-dependency of antiviral effect induced by IFN-β associated with that of IFNAR expression on liver. The fever induced by IFN-β showed a significant dosing time-dependent change, whereas the IFNAR expression on hypothalamus showed no significant diurnal rhythm. Furthermore, the rhythmic change of IFN-β pharmacokinetics failed to elucidate that of pharmacological effects induced by IFN-β, although there was a significant dosing time-dependent difference in plasma IFN-β concentrations. Previous study has shown that the interindividual variability in response of β-adrenoreceptor agonist or antagonist can be related to that in β-adrenoreceptor density on lymphocytes (Fraser et al., 1981, Zhou et al., 1989). Therefore, the choice of dosing time associated with the rhythmicity of IFNAR expression may help to achieve a rational chronopharmacological strategy for increasing the therapeutic effects of IFN-β. Also, the diurnal rhythm of IFNAR level on lymphocytes may be a reference marker for that of IFNAR level on liver, since IFNAR mRNA levels in both lymphocytes and liver exhibit similar rhythmicities. However, it is still unclear which factors control the rhythmicity of IFNAR expression. To clarify the mechanisms may lead to find out more convenient rhythmic marker for IFNAR expression in each tissue. From this question I might go on to a detailed examination of its mechanisms.

Table 3 Time-dependent difference of IFNAR expression on lymphocytes prepared at 17:00 or 5:00

IFNAR	Time of cell preparation (clock hours)		Student's t-test
	17:00	05:00	
Number (sites/cell)	218 ± 22	341± 29	P<0.01
Apparent Kd ($\times 10^{-10}$ M)	4.02 ± 0.39	4.43 ± 0.29	N.S.

Each value is the mean with S.E. of 5 mice.

Table 4 Influence of dosing time on plasma IFN-β concentrations after IFN-β (15MIU/kg, i.v.) injection at 09:00 or 21:00

Time after drug injection (hr)	Plasma IFN-β concentration (kIU/mL)		Student's t-test
	Time of drug injection (clock hours)		
	09:00	21:00	
0.167	59.014 ± 3.715	52.790 ± 3.980	N.S.
0.5	14.121 ± 0.674	12.906 ± 0.773	N.S.
1.0	6.048 ± 0.365	5.005 ± 0.371	N.S.
1.5	3.450 ± 0.241	2.688 ± 0.225	P<0.05
3.0	1.172 ± 0.113	0.789 ± 0.052	P<0.05

Each value is the mean with S.E. of 5 - 6 mice.

Table 5 Influence of dosing time on pharmacokinetic parameters after IFN-β (15MIU/kg, i.v.) injection at 09:00 or 21:00

Pharmacokinetic parameters		Time of drug injection (clock hours)		Student's t-test
		09:00	21:00	
CL	(L/hr/kg)	0.414 ± 0.012	0.484 ± 0.028	P<0.05
Vc	(L/kg)	0.106 ± 0.006	0.128 ± 0.547	N.S.
k_{12}	(1/hr)	1.783 ± 0.237	1.393 ± 0.124	N.S.
k_{21}	(1/hr)	1.199 ± 0.076	1.232 ± 0.041	N.S.

Each value is the mean with S.E. of 5-6 mice.

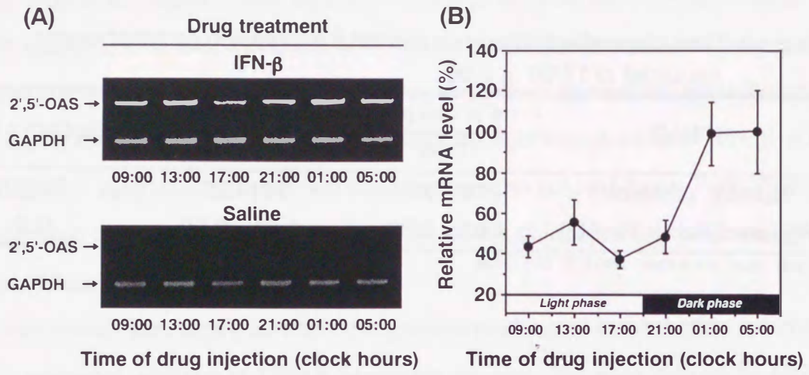

Fig.8 Diurnal rhythm of liver 2', 5'-OAS mRNA level at 4 hr after IFN-β (15 MIU/kg, i.v.) or saline injection at six different times. (A) Liver 2', 5'-OAS mRNA expression at 4 hr after IFN-β or saline injection. (B) Relative liver 2', 5'-OAS mRNA level (%) at 4 hr after IFN-β injection. Relative mRNA level sets the mean peak value of the rhythm at 100 %. Each values is the means with S.E. of 7 mice. Relative mRNA level showed a significant diurnal rhythm (P<0.01, ANOVA).

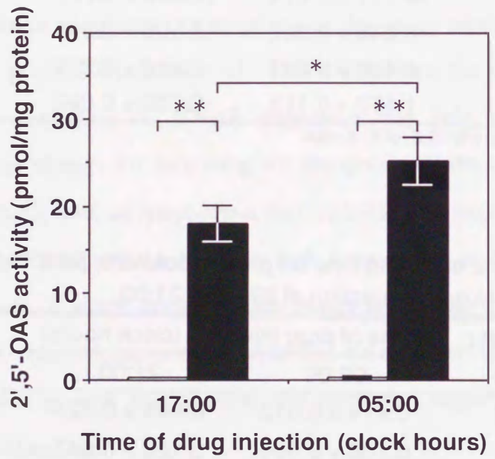

Fig.9 Influence of dosing time on liver 2', 5'-OAS activity at 12 hr after IFN-β (15 MIU/kg, i.v.)(■) or saline (□) injection. Each values is the means with S.E. of 7-8 mice. *P<0.05, **P<0.01 when compared with the corresponding saline group or between the two dosing times using Tukey's test.

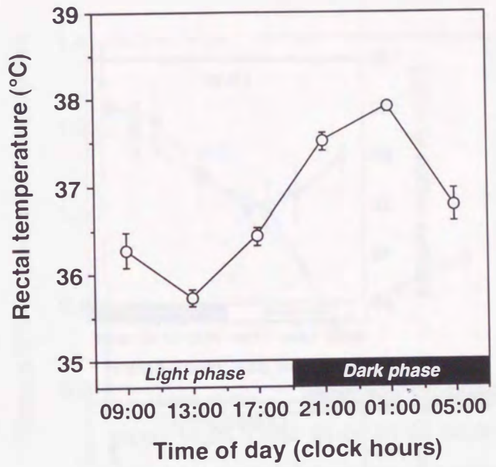

Fig.10 Diurnal rhythm of rectal temperature in mice at six different times. Each value is the mean with S.E. of 8 mice. Rectal temperature showed a significant diurnal rhythm (P<0.01, ANOVA).

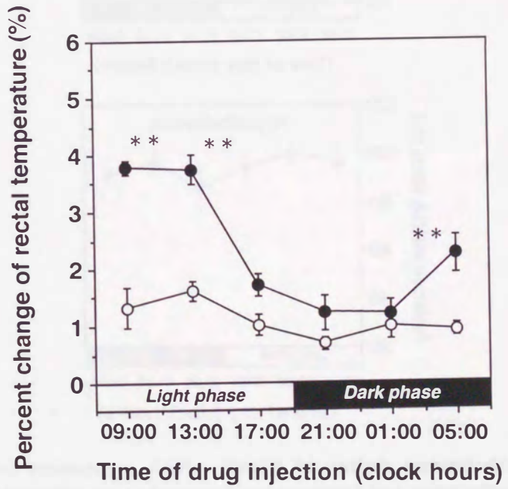

Fig.11 Diurnal rhythm of percent change of rectal temperature at 0.5 hr after IFN-β (15 MIU/kg, i.v.)(■) or saline (□) injection. Each value is the mean with S.E. of 6 mice. **P<0.01 when compared with the corresponding saline group using Tukey's test. A significant diurnal rhythm was demonstrated for IFN-β group (P<0.01, ANOVA)

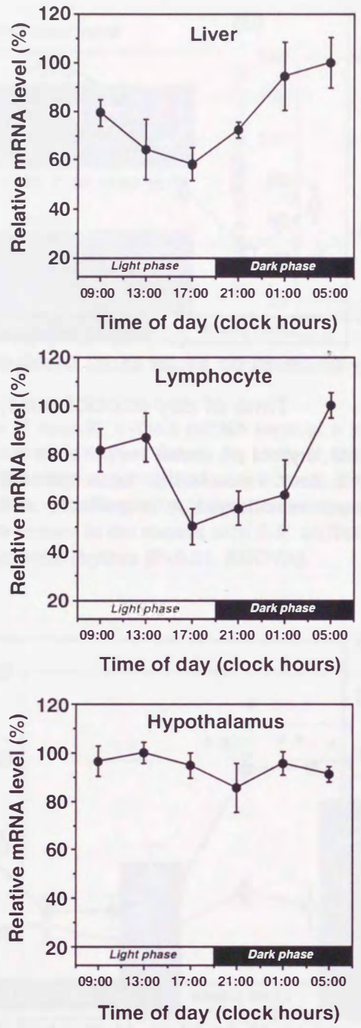

Fig.12 Diurnal rhythm of IFNAR mRNA expression in liver, hypothalamus and lymphocytes prepared at six different times. Relative mRNA level sets the mean peak value of each rhythm at 100 %, respectively. Each value is the mean with S.E. of 5 - 6 mice. A significant diurnal rhythm was demonstrated for liver and lymphocytes (P<0.01, respectively, ANOVA).

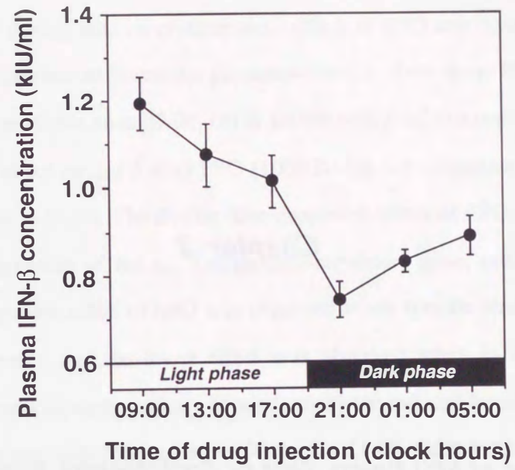

Fig.13 Diurnal rhythm of plasma IFN-β concentration at 2.5 hr after IFN-β (15 MIU/kg, i.v.) injection at six different times. Each value is the mean with S.E. of 5 - 6 mice. Plasma IFN-β concentrations showed a significant diurnal rhythm (P<0.01, ANOVA).

Chapter 2

Influence of EPO Dosing Time on Erythropoietic Effect in Mice

Abstract

The influence of dosing time on erythropoietic effect of EPO was investigated based on the sensitivity of bone marrow cells and the pharmacokinetics of the drug. Mice were housed in a light-controlled room (lights on at 07:00, off at 19:00) with food and water available *ad libitum*. The erythropoietic effect on day 5 after EPO (1000 IU/kg, s.c.) injection was more efficient at 13:00 or 01:00 than at 21:00. The dosing time-dependent effect of EPO was supported by the time-dependent expression of Bcl-x_L, antiapotosis-regulatory gene, mRNA induced by EPO. The higher erythropoietic effect of EPO was observed when specific binding of EPOR in bone marrow cells increased and the lower effect was observed when its levels decreased. The number of EPOR and erythroid colony formation activity induced by EPO were significantly higher in bone marrow cells obtained at 13:00 than at 21:00. On the other hand, there was no significant dosing time-dependent change in plasma EPO concentrations. Therefore, the time-dependent change of EPOR function seems to contribute to that of EPO-induced erythropoietic effect. The present results suggest that by choosing the most suitable dosing time for EPO, the efficacy of the drug can be increased in certain experimental and clinical situations.

Materials and Methods

Animals: Male ICR mice (5 weeks old) were purchased from the Charles River Japan Inç. (Kanagawa, Japan). They were housed 8 - 10 per cage under standardized light-dark cycle conditions (lights on at 07:00, off at 19:00) at 24 ± 1 ℃ and 60 ± 10 % humidity with food and water available *ad libitum*.

Drugs: The lyophilized powder of recombinant human EPO (Epogin®) (Chugai Pharmaceutical Co., Ltd., Tokyo, Japan) was dissolved in saline containing 0.05 % BSA and subcutaneously (s.c.) injected (0.1 ml/kg of body weight).

Experimental design: To investigate the influence of EPO dosing time on erythrocyte counts, groups of 5 - 9 mice were injected with EPO (1000 IU/kg, s.c.) or saline at once of six times: 09:00, 13:00, 17:00, 21:00, 01:00 or 05:00. Blood samples were collected by orbital sinus at the same time point (19:00) on day 5 after drug injection. To determine the influence of EPO dosing time on dose-response of EPO on erythrocyte counts, groups of 5 - 6 mice were injected subcutaneously with various dosage (0, 300, 1000 and 3000 IU/kg) of EPO at 13:00 or 21:00. Blood samples were collected by orbital sinus at the same time point (17:00) on day 5 after drug injection. To investigate the influence of EPO dosing time on Bcl-x_L mRNA level on bone marrow cells, groups of 5 - 6 mice were given a subcutaneous injection of EPO (1000 IU/kg) at 13:00 or 21:00. Bone marrow cells were collected at 4 hr after EPO injection. To examine the time-dependent change in sensitivity of bone marrow cells to EPO, bone marrow cells were obtained from groups of 7 mice at 13:00 or 21:00, and colony-forming units-erythroid (CFU-E) assay was performed described below. In order to study the diurnal rhythm of EPOR mRNA expression or specific EPO binding to EPOR on bone marrow cells, bone marrow cells were obtained from groups of 6 mice at each of the six times outlined above. Also, to investigate the time-dependent change of EPO binding sites or EPO affinity to EPOR on bone marrow cells, bone marrow cells were isolated from groups of 5 mice at 13:00 or 21:00 and specific EPO binding was evaluated by the scatchard analysis method described below. To determine the influence of EPO dosing time on time course of plasma EPO concentrations, groups of 5 mice were given a subcutaneous injection of EPO (1000 IU/kg) at

13:00 or 21:00. Blood samples were collected at 1, 3, 6, 8, 12, 16, 24, 36 or 48 hr after EPO injection.

Determination of erythrocyte counts: Blood samples were collected by orbital sinus on day 5 after EPO or saline injection. Erythrocyte number was measured using a Sysmex F-300 (Toua Iyou Denshi, Kobe, Japan). Percent increase of erythrocyte counts (%) from basal level in mice treated with saline was calculated as follows: % = ([erythrocyte counts after EPO injection – erythrocyte counts after saline injection] / [erythrocyte counts after saline injection]) × 100.

Bone marrow cells isolation: Mice were killed and their femurs were removed. Thereafter, femurs were flushed with 4 ml of phosphate-buffered saline (PBS) (2 ml from each end of the bone). The cell suspension was pooled and centrifuged at 1500 rpm for 10 min at 4 ℃. The pellets were washed twice with 2 ml of ice-cold PBS and then resuspended in medium for EPO binding assay.

RNA extraction and RT-PCR: Total RNA was extracted from bone marrow cells by using TRIZOL® solution (BRL, Bethesda, MD). The reverse transcription of RNA and cDNA amplification were perform with a one-step RT-PCR system (BRL). RT-PCR reactions were performed with Bcl-x_L, EPOR and glyceraldehyde-3-phosphate dehydrogenase (GAPDH) primers in a single tube. The following primers used: 5'-CTCTCCTACAAGCTTTCCCAG-3' and 5'-CCAGCGGTTGAAGCGCTCC-3' for Bcl-x_L (Gregory et al., 1999), 5'-CCGCATCA TCCATATCAATG-3' and 5'-AGACCCTCAAACTCGCTCTCTG-3' for EPOR (GenBank accession number; X04958) 5'-GACCTCAACTACATGGTCTACA-3' and 5'-ACTCCACGA CATACTCAGCAC-3' for GAPDH (GenBank accession number; M32599). The PCR product was electrophoresed through a 3 % agarose gel including 0.2 μg/ml ethidium bromide and the gel was photographed under UV light (302 nm). The mount of cDNA was quantified using a NIH image analysis program and normalized against GAPDH.

CFU-E assay: Bone marrow cells were extracted as described above and resuspended at a concentration of 10^5 cells/ml in D-MEM containing 0.8 % methylcellulose, 30 % heated-inactivated fetal bovine serum, 1 % BSA, 5×10^{-4} M mercaptoethanol, 0.5 % antibiotics (penicillin and streptomycin) and various concentrations (0.05 IU/ml) of EPO. The resuspended nucleated cells were then plated (1 ml / plate) onto 35-mm plastic tissue culture dishes. The cells were incubated for 7 days at 37 ℃ in a humidified atmosphere with 5 % CO_2. Colonies containing 8 or more cells were counted blindly by the same investigator using an inverted microscope.

EPOR binding assay: Isolated bone marrow cells were resuspended in ice-cold RPMI 1640 medium containing 2 % BSA, 0.2 % sodium azide, 25 mM HEPES and the indicated concentrations of [^{125}I]-EPO. The binding assay was performed at 37 ℃ for 1 hr with reaction mixture (a total volume 200 μl) containing various concentrations or 50 pM of [^{125}I]-EPO and 5×10^6 cells viable cells. After incubation, 300 μl of heated-inactivated fetal bovine serum was added and the mixture was centrifuged at 10000 rpm for 1 min. The supernatant was removed. Thereafter, the tube tip containing bound ligand was amputated and the radioactivity was measured using a gammer counter (ARC-360, Aloka Co., Mitaka, Tokyo, Japan). Nonspecific binding was evaluated in the presence of at least 400-fold excess of unlabeled EPO. Specific binding was defined as nonspecific binding subtracted from total binding. The data were plotted according to the method of Scatchard (Scatchard, 1949). A molecular weight of 30000 was assumed for the calculation of the receptor number per cell and the dissociation constant (Kd).

Determination of plasma EPO concentrations: Plasma samples were obtained after centrifugation at 3000 rpm for 3 min (Kubota Hematocrit KH-120A, Kubota, Tokyo, Japan) and stored at - 80 ℃ until assayed. Plasma EPO concentrations were determined by enzyme-immunoassay method (Immunoerit · EPO, Toyobo, Osaka, Japan).

Pharmacokinetic analysis: Pharmacokinetic parameters were calculated by the nonlinear least-squares method, following the one-compartment model: absorption rate constant (ka), elimination rate constant (ke), distribution volume / bioavailability (Vd / F), peak plasma concentration (Cmax), area under the curve (AUC) and mean residence time (MRT).

Statistical analysis: Analysis of variance (ANOVA) and Tukey's test were applied for the multiple comparison. Student's t-test was used for two independent groups. The 5 % level of probability was considered to be significant.

Results

Influence of EPO dosing time on erythropoietic effects.

In this experiments, all mice were bled at the same time point (17:00 or 19:00) on day 5 after drug injection, because of the erythrocyte counts showed a significant diurnal rhythm dependence in mice. The erythrocyte counts on day 5 after EPO (1000 IU/kg, s.c.) injection at other dosing times except 21:00 was significantly increased when compared with those after saline injection at corresponding dosing time ($P<0.01$, respectively, Fig.14). The erythrocyte-increasing effects of EPO showed a significant diurnal rhythm with higher level at 13:00 or 01:00 and trough level at 21:00. Also, the dosing time-dependent change of hemoglobin-increasing effect induced by EPO was consistent with that of the erythrocyte-increasing effect induced by EPO (data not shown).

Influence of EPO dosing time on dose-dependence of erythropoietic effects.

The increase of erythrocyte counts on day 5 after EPO (0 - 3000 IU/kg, s.c.) injection at 13:00 or 21:00 showed dose-dependent manner (Fig.15). A significant increase of erythrocyte counts was observed only in mice treated with a higher dose (1000 and 3000 IU/kg) of EPO at 13:00 ($P<0.01$, respectively), but not observed in mice treated with any dosage of EPO at 21:00. The degree of erythrocyte increase in mice injected with 3000 IU/kg of EPO at 21:00 was approximately agreed with that in mice injected with a dosage between 300 and 1000 IU/kg of EPO at 13:00. The similar results was observed for the dose-response effect of EPO on hemoglobin concentrations (data not shown).

Influence of EPO dosing time on Bcl-XL mRNA level in bone marrow cells.

As shown in Fig.16, the Bcl-XL mRNA level in bone marrow cells at 4 hr after EPO (1000 IU/kg, s.c.) injection at 13:00 was significantly higher when compared with that after saline injection at 13:00 ($P<0.05$). However, the mRNA level after EPO injection at 21:00 was not significantly different from that after saline injection.

Time-dependent change in erythroid colony formation by EPO in bone marrow cells.

The increase of erythroid colony induced by EPO showed dose-dependent manner (data not shown). Furthermore, there was a significant time-dependent difference in erythroid colony formation stimulated by EPO (0.05 IU/ml) in bone marrow cells (Fig.17). Number of colonies after EPO treatment was significantly higher in bone marrow cells prepared at 13:00 that at 21:00 ($P<0.05$).

Diurnal rhythm of EPOR expression on bone marrow cells.

The EPOR mRNA level in bone marrow cells prepared at six different times showed a significant diurnal rhythm ($P<0.01$, ANOVA, Fig.18 A). The mRNA level was higher at 13:00, 01:00 and 05:00 and lowest at 21:00. Next, we examined the diurnal rhythm of specific ^{125}I-EPO binding to EPOR on bone marrow cells. The binding assay was performed with 50 pM of [^{125}I]-EPO according to "Methods". The specific binding of ^{125}I-EPO to EPOR on bone marrow cells showed a significant diurnal rhythm ($P<0.01$, ANOVA, Fig.18 B). The binding showed a significant diurnal rhythm with first peak at 13:00 and then again peaking 01:00. Furthermore, the number of EPOR per cell on bone marrow cells, calculated from the intercept of the Scatchard plot on the abscissa, was significantly larger in cells prepared at 13:00 than at 21:00 ($P<0.01$, Table 6). The apparent Kd was not significantly different between the two sampling times.

Relationship between increase of erythrocyte counts by EPO and specific ^{125}I-EPO binding to bone marrow cells.

The relationship between the number of EPOR per cell and specific ^{125}I-EPO binding to bone marrow cells, based on the scatchard analysis data as shown in Table 6, is shown in Fig.19. The binding assay was performed with 50 pM of [^{125}I]-EPO according to "Methods". There was a significant positive correlation between the EPOR number and specific ^{125}I-EPO binding ($r=0.745$, $P<0.05$). Furthermore, the relationship between the percent increase of erythrocyte counts on day 5 after EPO (1000 IU/kg, s.c.) injection (See Fig.14) and specific ^{125}I-EPO binding to bone marrow cells (See Fig.18 B) is shown in Fig.20. There was a significant

positive correlation between specific ^{125}I-EPO binding and the increase of erythrocyte counts by EPO injection ($r=0.944$, $P<0.05$).

Influence of dosing time on EPO pharmacokinetics.

The influence of dosing time on time course of plasma EPO concentrations after (1000 IU/kg, s.c.) injection is shown in Fig.21. The plasma EPO concentration after EPO injection was reached a peak level from 8 to 12 hr after EPO injection and decreased in exponential fashion. Plasma EPO concentrations at any time after EPO injection at 13:00 showed no significant difference when compared with those after the drug injection at 21:00. Table 7 showed the pharmacokinetic parameters after EPO injection. The values of ka, ke, Vd / F, Cmax, AUC and MRT showed no significant difference between two dosing times.

Discussion

The erythrocyte or hemoglobin-increasing effects of EPO showed a significant diurnal rhythm with higher level at 13:00 or 01:00, and lower level at 21:00. This result was supported by a previous report (Wood et al., 1990). EPO promotes the survival and proliferation of erythroid progenitor in bone marrow through the induction of Bcl-x_L, antiapotosis-regulatory gene (Silva et al., 1996, Gregory and Bondurant, 1997). The Bcl-x_L mRNA level in bone marrow cells after EPO injection at 13:00 was significantly higher than that after saline injection. This result suggests that the dosing time-dependent change of EPO-induced antiapotic effects contributes to that of erythropoietic effects induced by the drug. Furthermore, I demonstrated the influence of dosing time on the relationship between dosage and erythropoietic effect of EPO. The erythrocyte or hemoglobin increasing effect in mice injected with 3000 IU/kg of EPO at 21:00 was approximately equivalent to that in mice injected with 500 IU/kg of EPO at 13:00.

The rhythmic change of drug response is caused by that of pharmacokinetic factors such as drug concentration at the site of action and/or pharmacodynamic factors such as receptor sensitivity to drug. The diurnal rhythm in myelosuppressive toxicity of anticancer drugs is closely related to that in cell cycle distribution of bone marrow cells (Ohdo et al., 1997b, Tampellini et al., 1998). The diurnal rhythm in sensitivity of bone marrow cells to G-CSF cause that of its leukocyte-increasing effect (Ohdo et al., 1998). EPO also stimulates proliferation and maturation of erythroid progenitors in bone marrow cells via binding to EPOR on cell surface.

First, I examined whether the sensitivity of bone marrow cells to EPO shows a diurnal rhythm. I observed that the specific EPO binding to bone marrow cells shows a significant diurnal rhythm with higher level at 13:00 or 01:00, and lower level at 21:00. The similar diurnal rhythmicity was observed in the EPOR mRNA level in bone marrow cells. Furthermore, the number of EPOR per cells was significantly larger in cells obtained at 13:00 than at 21:00. These results suggest that the diurnal rhythm dependence of transcriptional activity of EPOR mRNA, and its protein synthesis, contributes to that of EPOR density on bone marrow cells. Also, the diurnal rhythm of EPOR expression on bone marrow cells was consistent with that of

EPO erythropoietic effect. I observed a good positive correlation between the specific EPO binding to bone marrow cells and the erythrocyte increasing count after EPO injection. There was a positive correlation between the specific EPO binding to bone marrow cells and the EPOR number per cell. Thus, the diurnal rhythm of EPOR expression on bone marrow cells seems to be closely related to that of erythropoietic activity by EPO.

The burst-forming unit-erythroid and CFU-E, expressing high EPOR, are only EPO responsive erythroid progenitor in various bone marrow cell lineage (Broudy et al., 1991, Wickrema et al., 1992). For this reason the question I have to ask here is whether the diurnal rhythm of specific EPO binding to bone marrow cells is associated with that of EPOR expression per EPO responsive erythroid progenitor cells. In this study, the colony-forming activity of EPO was more potent in bone marrow cells prepared from mice at 13:00 than at 21:00. Namely, the diurnal rhythm in colony forming activity of EPO in vitro system was consistent with that in EPOR expression on bone marrow cells and that in erythropoietic effect of EPO in vivo. Also, the erythroid colony induced by EPO increased in a dose-dependent manner. These results suggest that the diurnal rhythm in specific EPO binding to bone marrow cells relates to that in number of EPOR per EPO responsive pre-erythroid cell.

The promoter region of human or mouse EPOR contains a binding site for GATA-1 and Sp1, positive transcriptional factor for EPOR (Youssoufian et al.,1990; Chin et al., 1995). GATA-1 exhibits specific expression in erythroid cells and is associated with the transcription activation of erythroid-expressed genes including globin (Orkin, 1992; Weiss and Orkin, 1995). It was found through our laboratory experiments that the mRNA level of GATA-1 shows a significant diurnal rhythm (data not shown). GATA-1 mRNA level oscillates with some advance in parallel to the rhythmicity of EPOR mRNA level in bone marrow cells. Therefore, the rhythmicity of EPOR mRNA level contributes to that of its protein synthesis and is regulated by, at least in part, that of positive transcriptional activation by GATA-1. Also, the half-life of EPOR mRNA in human or mouse is approximately 90 min or 75 min, respectively (Wickrema et al., 1991, 1992). These results and previous reports suggest that the metabolic turnover of EPOR is relatively rapid.

Next, I observed the influence of EPO dosing time dependence on plasma EPO concentration or its pharmacokinetic parameters after the drug injection. However, no significant dosing time-dependence was observed for EPO concentrations at any times after EPO injection. No significant dosing time-dependent difference was also demonstrated for ke and ka of EPO. A body clearance of EPO consists of saturable and nonsaturable clearances (Kato et al., 1997, 1998). The bone marrow cells and kidney mainly contribute to the saturable receptor-mediated uptake clearance and the nonsaturable glomerular filtration clearance, respectively. In this study, the number of EPOR per cell was significantly higher in bone marrow cells prepared at 13:00 than at 21:00. This result suggests that the saturable clearance of EPO is higher in mice injected with the drug at 13:00 than at 21:00. In human, the saturable clearance is predominant elimination pathway (Flaharty et al., 1990). However, the contribution of saturable clearance to body clearance is 30 % in rats (Kato et al., 1997), and smaller in mice than in rats (Kato et al., 1998). Therefore, the predominant pathway of EPO elimination in mice may be the kidney. The blood flow to kidney is significant diurnal rhythm with higher level during the dark phase and lower during the light phase (Labrecque et al., 1988). In this study, however, the plasma EPO concentrations after EPO injection showed no significant dosing time-difference between dosing times at 13:00 and 21:00. Also, there was no significant dosing time-dependent difference in Cmax, AUC as well as MRT. The finding showing no rhythmicity of pharmacokinetic parameters may be due to the slow elimination based on the slow absorption rate after EPO injection. Thus, EPO pharmacokinetics is not considered as the mechanism underlying the dosing time-dependent change of erythropoietic effects induced by EPO. It is possible that the diurnal rhythm of pharmacodynamic factors contributes to that of EPO pharmacological action.

In conclusion, I demonstrated the dosing time-dependent change in erythropoietic effect of EPO is caused by that of EPOR expression on bone marrow cells in mice. Also, the choice of EPO dosing time associated with the diurnal rhythm of EPOR expression may be one of cost-benefit approaches that can reduce the dosage of EPO with remaining its effect unaffected. EPO treatment is expensive, on the order of $10,000 per year for patient undergoing renal dialysis (Doolittle, 1991). Thus, these results suggest the usefulness of clinical chronotherapy with EPO for patients receiving EPO therapy.

Table 6 Time-dependent difference of EPOR expression on bone marrow cells prepared at 13:00 or 21:00

EPOR	Time of cell preparation (clock hours)		Student's t-test
	13:00	21:00	
Number (sites/cell)	24 ± 1	19 ± 2	P<0.01
Apparent Kd (pM)	124.726 ± 9.208	126.990 ± 9.310	N.S.

Each value is the mean with S.E. of 6 mice.

Table 7 Influence of dosing time on pharmacokinetic parameters after EPO(1000 IU/kg, s.c.) injection at 13:00 or 21:00

Pharmacokinetic parameters	Time of drug injection (clock hours)		Student's t-test
	13:00	21:00	
ka (hr^{-1})	0.174 ± 0.002	0.177 ± 0.002	N.S.
ke (hr^{-1})	0.161 ± 0.001	0.164 ± 0.001	N.S.
Vd/F (L/kg)	0.182 ± 0.010	0.174 ± 0.007	N.S.
Cmax (mIU/ml)	2130.447 ± 118.697	2179.154 ± 106.074	N.S.
AUC (mIU · hr/ml)	34577.150 ± 1819.515	34782.775 ± 1780.604	N.S.
MRT (hr)	11.957 ± 0.100	11.742 ± 0.096	N.S.

Each value is the mean with S.E. of 5 mice.

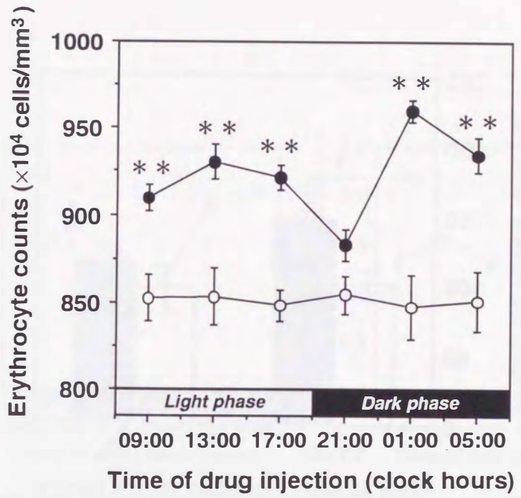

Fig.14 Influence of dosing time on erythrocyte counts after EPO (1000 IU/kg, s.c.)(●) or saline (○) injection. Each value is the mean with S.E. of 5 - 9 mice. Erythrocyte number was measured at 19:00 on day 5 after drug. **P<0.01 when compared with the saline group at corresponding dosing time using Tukey's test.

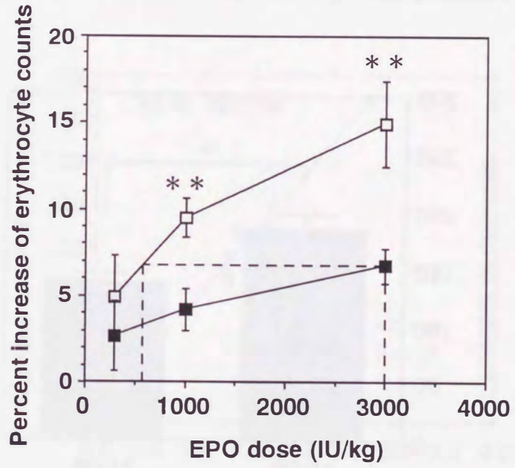

Fig.15 Influence of dosing time on dose-response effect on erythrocyte counts at day 5 after EPO injection at 13:00 (□) or 21:00 (■). Each value is the mean with S.E. of 5 - 6 mice. Erythrocyte number was measured at 17:00 on day 5 after drug injection. Percent increase change of erythrocyte counts induced by EPO was calculated as the percent change from mean value of mice injected with saline at 13:00 or 21:00. **P<0.01 when compared with the EPO group at 21:00 using Student's t-test.

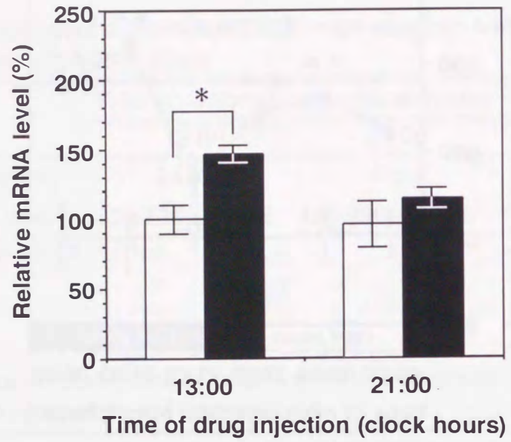

Fig.16 Influence of dosing time on Bcl-XL mRNA level in bone marrow cells at 4 hr after EPO (1000 IU/kg, s.c.)(■) or saline (□) injection. Relative mRNA level sets the mean value in mice injected with saline at 13:00 at 100 %. Each value is the mean with S.E. of 5 - 6 mice. *P<0.05 when compared with the corresponding saline group using Tukey's test.

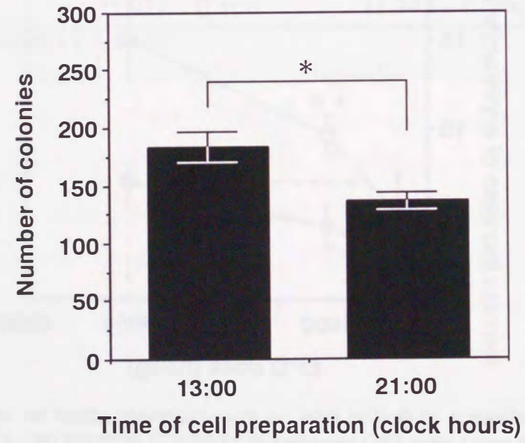

Fig.17 Time-dependent change of erythroid colony formation by EPO (0.05 IU/ml) in bone marrow cells. Each value is the mean with S.E. of 7 mice. *P<0.05 when compared between the two times using Student's t-test.

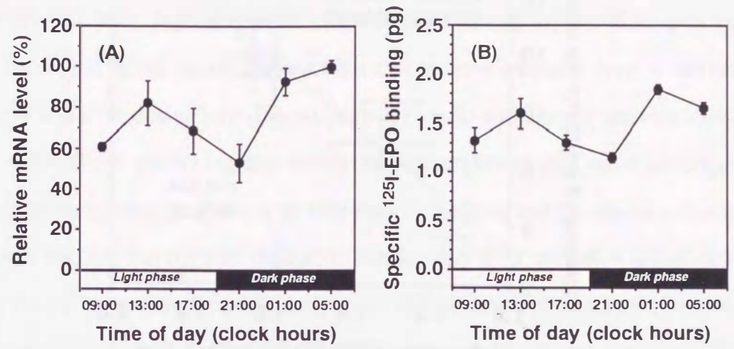

Fig.18 Diurnal rhythm of EPOR mRNA level (A) or specific ^{125}I-EPO binding (B) in EPOR in bone marrow cells prepared at six different times. Relative mRNA level sets the mean value at 05:00 at 100 %. Each value is the mean with S.E. of 6 mice. EPOR mRNA level and specific ^{125}I-EPO binding showed a significant diurnal rhythm (P<0.01, respectively, ANOVA).

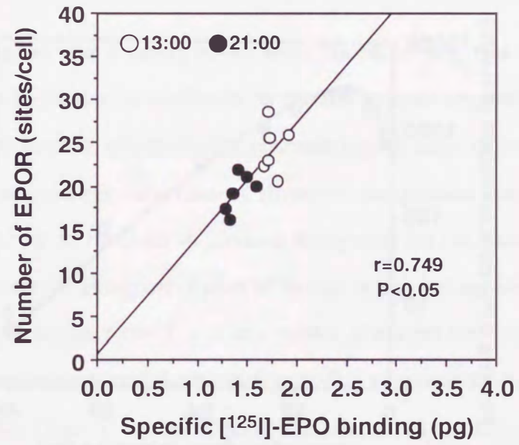

Fig.19 Correlation between number of EPOR on bone marrow cells and specific ^{125}I-EPO binding to the cells prepared at 13:00 or 21:00.

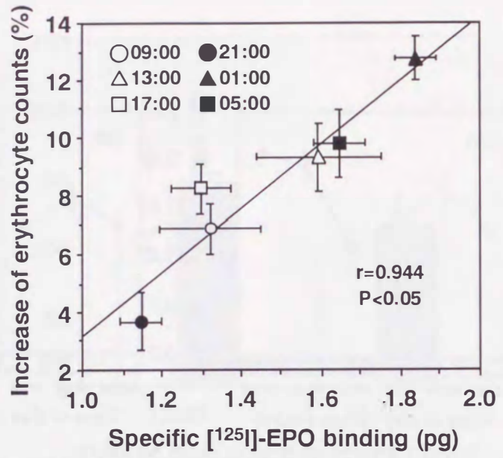

Fig.20 Correlation between diurnal rhythm in percent increase of erythrocyte counts on day 5 after EPO (1000 IU/kg, s.c.) injection and specific ^{125}I-EPO binding to bone marrow cells. Percent change of erythrocyte counts by EPO was calculated as the percent change from mean value of mice injected with saline at six different dosing times. Each value is calculated from Fig.14 or Fig.18 B, and is the mean with S.E. of 6 - 9 mice.

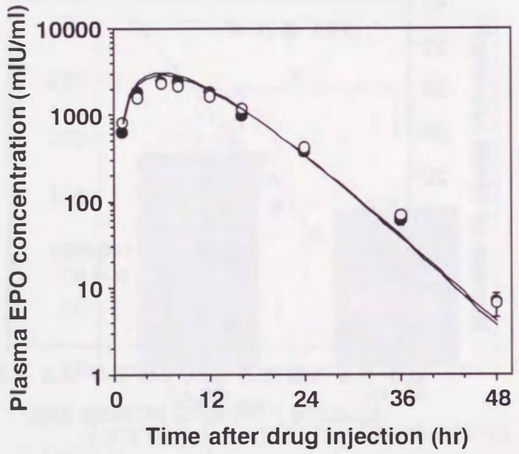

Fig.21 Influence of dosing time on time course of plasma EPO concentration after EPO (1000 IU/kg, s.c.) injection at 13:00 (○) or 21:00 (●). Each value is the mean with S.E. of 5 mice.

Summary

I have shown here the influence of dosing time on pharmacological effects of receptor-mediated drugs in mice, and the correlation between the diurnal rhythm of receptor expression on target tissue and that of pharmacological effect of receptor-mediated drug. In the first part of this paper, I found the dosing time-dependent change in the antitumor or antiviral effect of IFN-β. The mechanisms underlying the dosing time-dependent change were investigated from viewpoints of the sensitivity of tumor or liver cells to the drug and the pharmacokinetics of the drug. It was clarified that the time-dependent change of IFN-β antitumor or antiviral effect is related to that of the sensitivity, particularly at the IFNAR level, of tumor or liver cells to IFN-β. This study suggested that by choosing the most suitable dosing time for IFN-β, the efficacy of the drug can be increased. In the second part of this paper, I investigated the dosing time-dependent change in the erythropoietic effect of EPO, which is one of receptor-mediated drugs. The diurnal rhythm in erythropoietic effect of EPO was due to that in EPOR expression on bone marrow cells. Also, this study revealed that the choice of EPO dosing time associated with the diurnal rhythm of EPOR expression can reduce the dosage of EPO with leaving its effect unaffected.

These results suggest that a setting of the most suitable dosing time of receptor-mediated drugs, associated with the diurnal rhythm of its specific receptor expression on target tissues, may be important to increase effectively the pharmacological effect of the drug or reduce the dosage in experimental and clinical situations. However, the question remains when during the 24 hours treatments are to be timed to increase therapeutic benefit, since the interindividual variability may characterize biological rhythm of human beings but not laboratory animals. For example, although the serum cortisol, a strong marker of diurnal rhythm, shows a significant diurnal pattern with maximum level during early morning, a reversal diurnal rhythm is observed for night-shiftworker (Hennig et al., 1998). The diurnal rhythmicity of cortisol level is preserved in old age, but the timing of diurnal elevation is advanced (Van Cauter et al., 1996). Also, abnormal rhythmic patterns of serum cortisol is observed in breast and ovarian cancer patients (Touitou et al., 1996). Consequently, clinical situations need to incorporate monitoring of marker rhythm parameters in patients and individual adjustments of treatment schedules to

those rhythms. For the purpose, the future direction of this study should clarify the regulatory mechanism underlying dosing time-dependence of therapeutic efficacy. It may lead to the finding of reference marker to predict the rhythmicity of pharmacodynamics and/or pharmacokinetics

Circadian clock is made up of an input pathway, a control oscillator, and output pathway. The output pathways are likely to involve both nervous and humoral signals. Plasma endogenous glucocorticoid hormone level such as cortisol (human being) and corticosterone (rodents) shows a diurnal rhythmicity with elevation during early active phase. In the present study, the EPOR expression on bone marrow cells shows a significant diurnal rhythm with higher level at 13:00 or 01:00, and lower level at 21:00. The promoter region of human or mouse EPOR contains a binding site for GATA-1, positive transcriptional factor for EPOR (Youssoufian et al.,1990; Chin et al., 1995). The GATA-1 mRNA level was a significant diurnal rhythm associated with that temporal pattern of EPOR mRNA level in bone marrow cells (data not shown). Glucocorticoid inhibits not only the transcriptional activation of GATA-1-induced erythroid structural genes, but may also inhibit the expression of GATA-1 (Chang et al., 1993). Therefore, the diurnal rhythm of glucocorticoid hormone related to the transcriptional activation of EPOR may be able to explain that of EPOR expression, especially the trough level observed during early dark phase. It has been found through our laboratory experiments a possible mechanism underlying diurnal rhythm of IFNAR mRNA expression in peripheral tissues by glucocorticoid. Generally, exogenous glucocorticoid hormone influences cytokine production or its receptor expression such as IL-2 (Vacca et al., 1990), IL-1 receptor (Gottschall et al., 1991), IL-2 receptor (Lamas et al., 1997) and IL-6 receptor (Snyers et al., 1990). For example, IFN-γ production in lymphocytes is suppressed by glucocorticoid (Arya et al., 1984). There is an inverse relationship between the levels of plasma cortisol and IFN-γ production in antigen-stimulated lymphocytes (Petrovsky et al., 1994; Petrovsky and Harrison, 1997). Also, glucocorticoid enhanced the IFN-γ receptor expression (Strickland et al., 1986). The diurnal rhythm of IFN-γ receptor expression in SCN, the main pacemaker for diurnal rhythms, is observed in rat (Lundkvist et al., 1998). The expression of the receptor protein is dependent on light (Lundkvist et al., 1999). In the present study, IFNAR mRNA level in normal or tumor-bearing mice exhibits similar rhythmic pattern between the lymphocytes and

other peripheral tissues such as liver, tumor and kidney. Previous study reports that adrenergic receptor densities on lymphocytes reflect those on extravascular target tissues (Liggett et al., 1989). β-adrenoreceptor density on lymphocytes is significantly correlated to the response of β-adrenoreceptor agonist or antagonist (Fraser et al., 1981, Zhou et al., 1989). Therefore, the receptor expression on lymphocytes may be a useful candidate to predict the diurnal rhythm of receptor level on target tissue and the dosing time-dependent change in response of receptor-mediated drug.

This present study is the first report to suggest that IFNAR or EPOR expression on peripheral tissues shows a significant diurnal rhythm and the rhythmicity is closely related to the dosing time-dependent change in pharmacological effect of IFN-β or EPO. To monitor the rhythmicity of plasma glucocorticoid hormone level or receptor expression level on lymphocytes obtained from peripheral blood may be important to establish individually the dosing time for receptor-mediated drugs such as IFN-β or EPO to optimize chronotherapy (Fig.22). We should consider the background of individual patients such as the symptoms of disease and combined drug influencing receptor expression. Finally, this concept may be applicable to other receptor-mediated drugs as shown in the case of IFN-β and EPO.

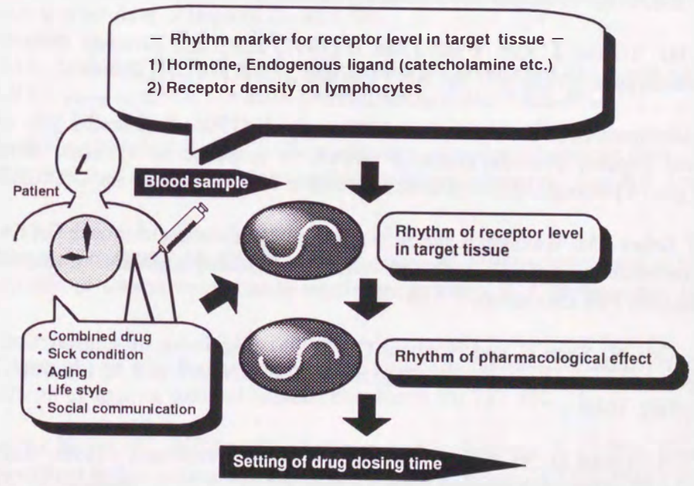

Fig.22 Prediction in the diurnal rhythm of receptor expression on target tissue in clinical situations

References

Arya SK, Wong-Staal F and Gallo RC (1984) Dexamethasone-mediated ihibition of human T cell growth factor and γ-interferon messenger RNA. J Immunol 133: 273-276.

Aschoff J (1963) Comparative physiology: Diurnal rhythms. Annu Rev Physiol 25: 581-600.

Baron S, Tyring S, Fleischmann WR, Coppenhaver DH, Niesel DW, Klimpel GR, Stanton GJ and Hughes K (1991) The interferons. JAMA 266: 1375-1383.

Blalock JE and Smith EM (1981) Human leukocyte interferon (HuIFN-α): potent endorphin-like opioid activity. Biochem Biophys Res Commu 101: 472-478.

Bocci V, Mogensen KE, Muscettola M, Pacini A, Paulesu L, Pessina GP and Skiftas S (1983) Degradation of human ^{125}I-interferon alpha by isolated perfused rabbit kidney and liver. J Lab Clin Med 101: 857-863.

Branca AA and Baglioni C (1981) Evidence that types I and II interferons have different receptors. Nature 294: 768-770.

Breymann C, Bauer C, Major A, Zimmermann R, Gautschi K, Huch A and Huch R (1996) Optimal timing of repeated rh-erythropoietin administration improves its effectiveness in stimulating erythropoiesis in healthy volunteers. Br J Haematol 92: 295-301.

Briese E, Hui-Wan H and Parada MA (1991) Stress hyperthermia in mice. J Therm Biol 16: 333-336.

Broudy VC, Lin N, Brice M, Nakamoto B and Papayannopoulou T (1991) Erythropoietin receptor characteristics on primary human erythroid cells. Blood 77: 2583-2590.

Burgess HJ, Trinder J, Kim Y and Luke D (1997) Sleep and circadian influences on cardiac autonomic nervous system activity. Am J Physiol 273: H1761-H1768.

Cao C, Matsumura K, Yamagata K and Watanabe Y (1996) Endothelial cells of the rat brain vasculature express cyclooxygenase-2 mRNA in response to systemic interleukin-1β: a possible site of prostaglandin synthesis responsible for fever. Brain Res 733: 263-272.

Chan TJ, Scher BM, Waxman S and Scher W (1993) Inhibition of mouse GATA-1 function by the glucocorticoid receptor: possible mechanism of steroid inhibition of erythroleukemia cell differentiation. Mol Endocrinol 7: 528-542.

Chin K, Oda N, Shen K and Noguchi CT (1995) Regulation of transcription of the human erythropoietin receptor gene by proteins binding to GATA-1 and Sp1 motifs. Nucleic Acids Res 23: 3041-3049.

Chin YE, Kitagawa M, Su WC S, You ZH, Iwamoto Y and Fu XY (1996) Cell growth arrest and induction of cyclin-dependent kinase inhibitor p21$^{WAF1/CIP1}$ mediated by STAT1. Science 272: 719-722.

Darnell JE Jr, Kerr IM and Stark GR (1994) Jak-STAT pathways and transcriptional activation in response to IFNs and other extracellular signaling proteins. Science 264: 1415-1421.

Davis GL, Balart LA, Schiff ER, Lindsay K, Bodenheimer HC and Perrillo RP (1989) Treatment for chronic hepatitis C with recombinant interferon alpha: a multicenter randmized controlled trial. N Engl J Med 321:1501-1506.

Davis ME, Akera T and Brody TM (1979) Reduction of opiate binding to brain stem slices associated with the development of tolerance to morphine in rats. J Pharmacol Exp Ther 211: 112-119.

Diaz-Guerra M, Rivas C and Esteban M (1997) Inducible expression of the 2-5A synthetase/RNase L system results in inhibition of vaccinia virus replication. Virology 227: 220-228.

Doolittle RF (1991) Biotechnology. the enormous cost of success. N Engl J Med 324: 1360-1362.

Eschbach JW, Kelly MR, Haley NR, Abels RI and Adamson JW (1989) Treatment of the anemia of progressive renal failure with recombinant human erythropoietin. N Engl J Med 321: 158-163.

Flaharty KK, Caro J, Erslev A, Whalen JJ, Morris EM, Bjornsson TD and Vlasses PH (1990) Pharmacokinetics and erythropoietic response to human recombinant erythropoietin in healthy men. Clin Pharmacol Ther 47: 557-564.

Fraser J, Nadeau J, Robertson D and Wood AJJ (1981) Regulation of human leukocyte β-receptors by endogenous catecholamies: relationship of leukocyte β-receptor density to the cardiac sensitivity to isoproterenol. J Clin Invest 67: 1777-1784.

Fukuda R, Ishimura N, Kushiyama Y, Moriyama N, Ishihara S, Nagasawa S, Miyake T, Niigaki M, Satoh S, Sakai S, Akagi S, Watanabe M and Fukumoto S (1997) Effectiveness of interferon-alpha therapy in chronic hepatitis C is associated with the amount of interferon-alpha receptor mRNA in the liver. J Hepatol 26: 455-461.

Goldberg MA, Dunning SP and Bunn HF (1988) Regulation of the erythropoietin gene: evidence that the oxygen sensor is a heme protein. Science 242: 1412-1415.

Goldenheim PD and Schein LK (1992) Chronotherapy of reversible airways disease with once-daily evening doses of a controlled-release theophylline preparation. Ann NY Acad Sci 618: 490-503.

Gomi K, Kimura H, Okabe M, Oka T and Morimoto M (1986) Synergistic anticellular and antiviral activities of human recombinant interferon-γ and -β. J Pharmacobio Dyn 9: 871-878.

Gomi K, Morimoto M and Nakamizo N (1983) Growth-inhibitory activity of recombinant human interferon-β against cultured human cells. Gann 74: 737-742.

Gottschall PE, Koves K, Mizuno K, Tatsuno I and Arimura A (1991) Glucocorticoid upregulation of interleukin 1 receptor expression in a glioblastoma cell line. Am J Physiol 261: E362-E368.

Gregoli PA and Bondurant MC (1997) The roles of Bcl-X_L and apopain in the control of erythropoiesis by erythropoietin. Blood 90: 630-640.

Hennig J. Kieferdorf P. Moritz C. Huwe S and Netter P (1998) Changes in cortisol secretion during shiftwork: implications for tolerance to shiftwork?. Ergonomics 41:610-621.

Hori K, Zhang QH, Li HC and Saito S (1995) Variation of growth rate of a rat tumour during a light-dark cycle: correlation with circadian fluctuations in tumour blood flow. Br J Cancer 71: 1163-1168.

Hrushesky WJM (1985) Circadian timing of cancer chemotherapy. Science 228: 73-75.

Hunter T and Pines J (1994) Cyclins and cancer II: Cyclin D and CDK inhibitors come of age. Cell 79: 573-582.

Hwang SY, Hertzog PJ, Holland KA, Sumarsono SH, Tymms MJ, Hamilton JA, Whitty G, Bertoncello I and Kola I (1995) A null mutation in the gene encoding a type I interferon receptor component eliminates antiproliferative and antiviral responses to interferons α and β and alters macrophage responses. Proc Natl Acad Sci USA 92: 11284-11288.

Ida N, Uenishi N, Kajita A and Satoh Y (1982) Antitumor effect of human fibroblast interferon on the growth of human melanoma cells implanted in nude mice. Gann 73: 952-960.

Kafka MS, Benedito MA, Blendy JA and Tokola NS (1986) Circadian rhythms in neurotransmitter receptors in discrete rat brain regions. Chronobiol Int 3: 91-100.

Kafka MS, Marangos PJ and Moore RY (1985) Suprachiasmatic nucleus ablation abolishes circadian rhythms in rat brain neurotransmitter receptors. Brain Res 327: 344-347.

Kafka MS, Wirz-Justice A and Naber D (1981) Circadian and seasonal rhythms in alpha- and beta-sdrenergic receptors in the rat brain. Brain Res 207: 409-419.

Kanai K, Kako M and Okamoto H (1992) HCV genotypes in chronic hepatitis C and response to interferon. Lancet 339: 1543.

Kato M, Kamiyama H, Okazaki A, Kumaki K, Kato Y and Sugiyama Y (1997) Mechanism for the nonlinear pharmacokinetics of erythropoietin in rats. J Pharmacol Exp Ther 283: 520-527.

Kato M, Miura K, Kamiyama H, Okazaki A, Kumaki K, Kato Y and Sugiyama Y (1998) Pharmacokinetics of erythropoietin in genetically anemic mice. Drug Metab Dispos 26: 126-131.

Kavaliers M and Hirst M (1983) Daily rhythms of analgesia in mice: effects of age and photoperiod. Brain Res 279: 387-393.

Koren S and Fleischmann WR (1993) Circadian variations in myelosuppressive activity of interferon-α in mice: Identification of an optimal treatment time associated with reduced myelosuppressive activity. Exp Hematol 21: 552-559.

Koren S, Whorton EB and Fleischmann WR (1993) Circadian dependence of interferon antitumor activity in mice. J Natl Cancer Int 85: 1927-1932.

Koyanagi S, Ohdo S, Yukawa E and Higuchi S (1997) Chronopharmacological study of interferon-α in mice. J Pharmacol Exp Ther 283: 259-264.

Kumar R, Choubey D, Lengyel P and Sen GC (1988) Studies on the role of the 2'-5'-oligoadenylate synthetase-RNase L pathway in beta interferon-mediated inhibition of encephalomyocarditis virus replication. J Virol 62: 3175-3181.

Kumar R, Korutla L and Zhang K (1994) Cell cycle-dependent modulation of α-interferon-inducible gene expression and activation of signaling components in Daudi cells. J Biol Chem 269: 25437-25441.

Kushnaryov VM, MacDonald HS, Sedmak JJ and Grossberg SE (1985) Murine interferon-β receptor-mediated endocytosis and nuclear membrane binding. Proc Natl Acad Sci USA 82: 3281-3285.

Kuwabara T, Kato Y, Kobayashi S, Suzuki H and Sugiyama Y (1994) Nonlinear pharmacokinetics of a recombinant human granulocyte colony-stimulating factor derivative (nartograstim): species differences among rats, monkeys and humans. J Pharmacol Exp Ther 271: 1535-1543.

Labrecque G, Bélanger PM, Doré F and Lalande M (1988) 24-Hour variations in the distribution of labeled microspheres to the intestine, liver and kidneys. Ann Rev Chronopharmacol 5: 445-448.

Lamas M, Campos JR and Silva AG (1997) Identification of a novel glucocorticoid response unit (GRU) in the 5'-flanking region of the mouse IL-2 receptor α gene. Cytokine 9: 973-981.

Lau JYN, Sheron N, Morris AG, Bomford AB, Alexander GJM and Williams R (1991) Interferon-α receptor expression and regulation in chronic hepatitis B virus infection. Hepatology 13: 332-338.

Lengyel P (1982) Biochemistry of interferons and their actions. Annu Rev Biochem 51:251-282.

Lévi F, Canon C, Dipalma M, Florentin I and Misset JL (1991) When should the immune clock be reset ?. Ann NY Acad Sci 518:312-329.

Lévi F, Zidani R and Misset JL (1997) Randomised multicentre trial of chronotherapy with oxaliplatin, fluorouracil, and folinic acid in metastatic colorectal cancer. Lancet 350: 681-686.

Levy DE, Kessler DS, Pine R and Darnell JE Jr (1989) Cytoplasmic activation of ISGF3, the positive regulator of interferon-α-stimulated transcription, reconstituted in vitro. Genes Dev 3: 1362-1371.

Lin R, Roach R, Zimmerman M, Strasser S and Farrel G (1995) Interferon alpha-2b for chronic hepatitis C: effectss of dose increment and duration of treatment on response rates. J Hepatol 23:487-496.

Lundkvist GB, Andersson A, Robertson B, Rottenberg ME and Kristensson K (1999) Light-dependent regulation and postnatal development of the interferon-γ receptor in the rat suprachiasmatic nuclei. Brain Res 849: 231-234.

Lundkvist GB, Robertson B, Mhlanga JDM, Rottenberg ME and Kristensson K (1998) Expression of an oscillating interferon-γ receptor in the suprachiasmatic nuclei. NeuroReport 9: 1059-1063.

Mandal M, Bandyopadhyay D, Goepfert TM and Kumar R (1998) Interferon-induces expression of cyclin-dependent kinase-inhibitors $p21^{WAF1}$ and $p27^{Kip1}$ that prevent activation of cyclin-dependent kinase by CDK-activating kinase (CAK). Oncogene 16: 217-225.

Masferrer JL, Reddy ST, Zweifel BS, Seibert K, Needleman P, Gilbert RS and Herschman HR (1994) In vivo glucocorticoids regulate cyclooxygenase-2 but not cyclooxygenase-1 in peritoneal macrophages. J Pharmacol Exp Ther 270: 1340-1344.

McMahon FG, Vargas R, Ryan M, Jain AK, Abels RI, Perry B and Smith IL (1990) Pharmacokinetics and effects of recombinant human erythropoietin after intravenous and subcutaneous injections in healthy volunteers. Blood 76: 1718-1722.

Mizukoshi E, Kaneko S, Yanagi M, Ohno H, Kaji K, Terasaki S, Shimoda A, Matsushita E and Kobayashi K (1998) Expression of interferon alpha/beta receptor in the liver of chronic hepatitis C patients. J Med Virol 56:217-223.

Naber D, Wirz-Justice A and Kafka MS (1981) Circadian rhythm in rat brain opiate receptor. Neurosci Lett 21: 45-50.

Naber D, Wirz-Justice A, Kafka MS and Wehr TA (1980) Dopamine receptor binding in rat striatum: ultradian rhythm and its modification by chronic imipramine. Psychopharmacol 68: 1-5.

Nakashima T, Hori T, Kuriyama K and Matsuda T (1988) Effects of interferon-α on the activity of preoptic thermosensitive neurons in tissue slices. Brain Res 454: 361-367.

Nakashima T, Murakami T, Murai Y, Hori T, Miyata S and Kiyohara T (1995) Naloxone suppresses the rising phase of fever induced by interferon-α. Brain Res Bull 37:61-66.

Novick D, Cohen B and Rubinstein M (1994) The human interferon α/β receptor: characterization and molecular cloning. Cell 77: 391-400.

Ohdo S, Arata N, Furukubo T, Yukawa E, Higuchi S, Nakano S and Ogawa N (1998) Chronopharmacology of granulocyte colony-stimulating factor in mice. J Pharmacol Exp Ther 285: 242-246.

Ohdo S, Grass GM and Lee VHL (1991) Improving the ocular to systemic ratio of topical timolol by varying the dosing time. Invest Ophthalmol Vis Sci 32: 2790-2798.

Ohdo S, Koyanagi S, Yukawa E and Higuchi S (1997a) Circadian rhythm of fever induced by interferon-α in mice. Life Sci 61: PL95-100.

Ohdo S, Makinosumi T, Ishizaki T, Yukawa E, HIguchi S and Nakano S (1997b) Cell cycle-dependent chronotoxicity of irinotecan hydrochloride in mice. J Pharmacol Exp Ther 283: 1383-1388.

Ohdo S, Nakano S and Ogawa N (1988) Chronopharmacological study of sodium valproate in mice: Dose-concentration-response relationship. Jpn J Pharmacol 47: 11-19.

Ohdo S, Ogawa N, Nakano S and Higuchi S (1996) Influence of feeding schedule on the chronopharmacological aspects of sodium valproate in mice. J Pharmacol Exp Ther 278: 74-81.

Orkin SH (1992) GATA-binding transcription factors in hematopoietic cells. Blood 80: 575-581.

Petrovsky N and Harrison LC (1997) Diurnal rhythmicity of human cytokine production. a dynamic disequilibrium in T helper cell type 1/T helper cell type 2 balance ?. J Immunol 158: 5163-5168.

Petrovsky N, McNair P and Harrison LC (1994) Circadian rhythmicity of interferon-gamma production in antigen-stimulated whole blood. Chronibiologia 21: 293-300.

Qureshi SA, Salditt-Georgieff M and Darnell JE Jr (1995) Tyrosine-phosphorylated Stat1 and Stat2 plus a 48-kDa protein all contact DNA in forming interferon-stimulated-gene factor 3. Proc Natl Acad Sci USA 92: 3829-3833.

Refinetti R and Menaker M (1992) The circadian rhythm of body temperature. Physiol Behavior 51: 613-637.

Rivington RN, Calcutt L, Child S, MacLeod JP, Hodder RV and Stewart JH (1985) Comparison of morning versus evening dosing with a new once-daily oral theophylline formulation. Am J Med 79 (suppl 6A): 67-72.

Sangfelt O, Erickson S, Einhorn S and Grandér D (1997): Induction of Cip/Kip and Ink4 cyclin dependent kinase inhibitors by interferon-α in hematopoietic cell lines. Oncogene 14: 415-423.

Scatchard G (1949) The attraction of protein for small molecules and ions. Ann NY Acad Sci 51: 660-672.

Silva M, Grillot D, Benito A, Richard C, Nuñez G and Fernández-Luna JL (1996) Erythropoietin can promote erythroid progenitor survival by repressing apotosis through Bcl-X_L and Bcl-2. Blood 88: 1576-1582.

Snyers L, Wit LD and Content J (1990) Glucocorticoid up-regulation of high-affinity interleukin 6 receptors on human epithelial cells. Proc Natl Acad Sci USA 87: 2838-2842.

Sokawa Y, Kitano Y, Shimada M, Okumura M, Sokawa J, Ueda K, Hamada K and Takeda K (1994) Physiological expression of the 2'-5' oligoadenylate synthetase gene in mouse intestine. J Interferon Res 14: 121-127.

Strickland RW, Wahl LM and Finbloom DS (1986) Corticosteroids enhance the binding of recombinant interferon-γ to cultured human monocytes. J Immunol 137: 1577-1580.

Sun WH, Pabon C, Alsayed Y, Huang PP, Jandeska S, Uddin S, Platanias LC and Rosen ST (1998) Interferon-α resistance in a cutaneous T-cell lymphoma cell line is associated with lack of STAT1 expression. Blood 91: 570-576.

Tampellini M, Filipski E, Liu XH, Lemaigre G, Li XM, Vrignaud P, Francois E, Bissery MC and Lévi F (1998) Docetaxel chronopharmacology in mice. Cancer Res 58: 3896-3904.

Tamura T, Matsuzaki M, Harada H, Ogawa K, Mohri H and Okubo T (1997) Upregulation of interferon-α receptor expression in hydroxyurea-treated leukemia cell lines. J Invest Med 45: 160-167.

Thornton AM, Ogryzko VV, Dent A, Sharf R, Levi BZ, Kanno Y, Staudt LM, Howard BH and Ozato K (1996) A dominant negative mutant of an IFN regulatory factor family protein inhibits both type I and type II IFN-stimulated gene expression and antiproliferative activity of IFNs. J Immunol 157: 5145-5154.

Touitou Y, Bogdan A, Levi F, Benavides M and Auzeby A (1996) Distribution of the circadian patterns of serum cortisol in breast and ovarian cancer patients: relationships with tumour marker antigens. Br J Cancer 74: 1248-1252.

Toyoda H, Kumada T, Nakano S, Takeda I, Sugiyama K, Osada T, Kiriyama S, Sone Y, Kinoshita M and Hadama T (1997) Quasispecies nature of hepatitis C virus and response to alpha interferon: significance as a predictor of direct response to interferon. J Hepatol 26: 6-13.

Vacca A, Martinotti S, Screpanti I, Maroder M, Felli MP, Farina AR, Gismondi A, Santoni A, Frati L and Gulino A (1990) Transcriptional regulation of the interleukin 2 gene by glucocorticoid hormones. J Biol Cem 265: 8075-8080.

Van Cauter E. Leproult R and Kupfer DJ (1996) Effects of gender and age on the levels and circadian rhythmicity of plasma cortisol. J Clin Endocrinol Metab 81:2468-2473.

Warner CW and McIsaac RL (1992) The evolution of peptic ulcer therapy. A role for temporal control of drug delivery. Ann NY Acad Sci 618: 504-516.

Watanabe H, Ohdo S, Ishikawa M and Ogawa N (1992) Effects of social isolation on pentobarbital activity in mice: Relationship to racemate levels and enantiomers levels in brain. J Pharmacol Exp Ther 263: 1036-1045.

Weiss MJ and Orkin SH (1995) GATA transcription factors: key regulators of hematopoiesis. Exp Hematol 23: 99-107.

Wickrema A, Bondurant MC and Krantz SB (1991) Abundance and stability of erythropoietin receptor mRNA in mouse erythroid progenitor cells. Blood 78: 2269-2275.

Wickrema A, Krantz SB, Winkelmann JC and Bondurant MC (1992) Differentiation and erythropoietin receptor gene expression in human erythroid progenitor cells. Blood 80: 1940-1949.

Wills RJ (1990) Clinical pharmacokinetics of interferons. Clin Pharmacokinet 19:390-399.

Wirz-Justice A, Kafka MS, Naber D, Campbell IC, Marangos PJ, Tamarkin L and Wehr TA (1982) Clorgyline delays the phase-position of circadian neurotransmitter receptor rhythms. Brain Res 241: 115-122.

Wirz-Justice A, Kafka MS, Naber D, Marangos PJ, Tamarkin L O'Donohue TL and Wehr TA (1982) Effect of lithium on circadian neurotransmitter receptor rhythms. Neuropsychobiol 8: 41-50.

Wirz-Justice A, Kafka MS, Naber D and Wehr TA (1980) Circadian rhythms in rat brain alpha- and beta- adrenergic receptors are modified by chronic imipramine. Life Sci 27: 341-347.

Wong VLY, Rieman DJ, Aronson L, Dalton BJ, Greig R and Anzano MA (1989) Growth-inhibitory activity of interferon-beta against human colorectal carcinoma cell lines. Int J Cancer 43: 526-530.

Wood PA, Sánchez de la Peña S and Hrushesky WJM (1990) Circadian timing of recombinant human erythropoietin (rhEPO) in the mouse affects hematopoietic response. Ann Rev Chronopharmacol 7: 173-176.

Yamada H and Shimoyama M (1983) Growth inhibitory activity of human lymphoblastoid and fibroblast interferons in vitro. Gann 74: 299-307.

Yatsuhashi H, Fujino T, Matsumoto T, Inoue O, Koga M and Yano M (1999) Immunohistochemical analysis of hepatic interferon alpha-beta receptor level: relationship between receptor expression and response to interferon therapy in patients with chronic hepatitis C. J Hepatol 30:995-1003.

Youssoufian H, Zon LI, Orkin SH, D'Andrea AD and Lodish HF (1990) Structure and transcription of the mouse erythropoietin receptor gene. Mol Cell Biol 10: 3675-3682.

Yucel-Lindberg T, Ahola H, Nilsson S, Carlstedt-Duke J and Modeer T (1995) Interleukin-1 beta induces expression of cyclooxygenase-2 mRNA in human gingival fibroblasts. Inflammation 19: 549-560.

Zhou HH, Silberstein DJ, Koshakji RP and Wood AJJ (1989) Interindividual differences in β -receptor density contribute to variability in response to β-adrenoceptor antagonists. Clin Pharmacol Ther 45: 587-592.

Zoon KC and Arnheiter H (1984) Studies of the interferon receptors. Pharmacol Ther 24: 259-278.